Supplementary Materials for

Dengue viruses cluster antigenically but not as discrete serotypes

Authors: Leah C. Katzelnick, Judith M. Fonville, Gregory D. Gromowski, Jose Bustos Arriaga, Angela Green, Sarah L. James, Louis Lau, Magelda Montoya, Chunling Wang, Laura A. VanBlargan, Colin A. Russell, Hlaing Myat Thu, Theodore C. Pierson, Philippe Buchy, John G. Aaskov, Jorge L. Muñoz-Jordán, Nikos Vasilakis, Robert V. Gibbons, Robert B. Tesh, Albert D.M.E. Osterhaus, Ron A.M. Fouchier, Anna Durbin, Cameron P. Simmons, Edward C. Holmes, Eva Harris, Stephen S. Whitehead, Derek J. Smith*

* Corresponding author. E-mail: Derek Smith (djs200@cam.ac.uk).

This PDF file includes:

Materials and Methods
Supplementary Text
Figs. S1 to S29
Tables S1 to S15

Other Supplementary Materials for this manuscript includes the following:

Data files S1 to S9 as zipped archives:

Alignment of E nucleotide sequences for Fig. 1A
PhyML tree for Fig. 1A
Bootstrap trees for Fig. 1A
Sequence name key for Fig. 1A
Alignment of E nucleotide sequences for fig. S1
PhyML tree for fig. S1
Bootstrap trees for fig. S1
Sequence name key for fig. S1
Excel file including tables S3 – S7

Table of Contents

Figures and Tables

1. Methods

1.1. The DENV panel

1.1.1. Selection of isolates

In total, a panel of 47 viruses was assembled for antigenic characterization. The viruses were selected to represent geographic (20 countries), temporal (years 1944-2012), and genetic diversity (representatives of known genotypes of DENV isolated to date are included: table S1; Fig. 1; and fig. S1). The sample was designed to capture a wide range of antigenic diversity. However, it is possible that when more DENV isolates are tested in future studies, the scope of antigenic variation within and among types may be greater than that observed in this study.

DENV Type	Location	Year	GenBank identity number	Genotype: Holmes and Twiddy nomenclature	Genotype: Rico-Hesse nomenclature	Identity number	Used for NHP infection	One- month NHP map	Three- month NHP map	Five- month NHP map	Human mono- valent vaccine map	Human natural infection map
1	Bolivia	2010	KT382187	V	Americas-Africa	FSB-3363	Yes	Yes	Yes	Yes	Yes	
1	Myanmar	2005	KT452791	I	Asian	61117	Yes	Yes	Yes			
1	Cambodia	2003	GQ868619	I	Asian	BID-V1991	Yes	Yes	Yes			Yes
1	Cambodia	2003	FJ639680	I	Asian	BID-V1995		Yes	Yes	Yes	Yes	
1	Nauru	1974	AY145121	IV	South Pacific	WestPac	Yes	Yes	Yes	Yes	Yes	
1	Peru	2000	AY780643	V	Americas-Africa	IQT-6152	Yes	Yes	Yes			
1	Puerto Rico	2006	EU482591	V	Americas-Africa	BID-V852	Yes	Yes	Yes	Yes	Yes	Yes
1	Thailand	1964	AF180817	II	Thailand	16007	Yes	Yes	Yes	Yes	Yes	Yes
1	Venezuela	2000	KT382186	V	Americas-Africa	OBT-1298	Yes	Yes	Yes	Yes	Yes	
1	Vietnam	2008	FJ461335	I	Asian	BID-V1937	Yes	Yes	Yes	Yes	Yes	Yes
2	Brazil	2004	KT382189	Asian/American	Southeast Asia	BR-161		Yes	Yes	Yes	Yes	
2	Cambodia	2009	KT452795	Asian I	Southeast Asia	D2T0601085_KH09_KSP	Yes	Yes	Yes			
2	Cambodia	2007	GU131927	Asian I	Southeast Asia	BID-V4265		Yes	Yes	Yes	Yes	
2	Cambodia	2008	GQ868638	Asian I	Southeast Asia	BID-V3924		Yes	Yes	Yes	Yes	
2	Guyana	2000	KT382188	Asian/American	Southeast Asia	CAREC-00-08221		Yes	Yes	Yes	Yes	Yes
2	India	1974	FJ538920	Cosmopolitan	Malaysia/Indian Subcontinent	Poona-742295		Yes	Yes	Yes	Yes	
2	Malaysia	2008	FJ467493	Sylvatic	Malaysian	DKD-811	Yes	Yes	Yes	Yes	Yes	Yes
2	New Guinea	1944	AF038403	Asian II	Southeast Asia	New Guinea C		Yes	Yes	Yes	Yes	
2	Nicaragua	2005	EU482756	Asian/American	Southeast Asia	BID-V533	Yes	Yes	Yes	Yes	Yes	
2	Nicaragua	2006	EU482684	Asian/American	Southeast Asia	BID-V571	Yes	Yes	Yes	Yes	Yes	
2	Peru	1996	AY158339	American	American	IQT-2913	Yes	Yes	Yes	Yes	Yes	
2	Senegal	1970	EF105384	Sylvatic	Sylvatic	Sendak_H D_0674	Yes	Yes	Yes			
2	Tonga	1974	AY744147	American	American	Tonga/74	Yes	Yes	Yes	Yes	Yes	Yes
2	Vietnam	2003	KT452797	Asian/American	Southeast Asia	DF670-AC20	Yes	Yes	Yes	Yes	Yes	
2	Vietnam	2003	KT452796	Asian/American	Southeast Asia	AC21	Yes (2)	Yes	Yes	Yes	Yes	Yes
2	Vietnam	2006	EU482672	Cosmopolitan	Malaysia/Indian Subcontinent	32-135	Yes (2)	Yes	Yes	Yes	Yes	
3	Myanmar	2008	KT452792	II	Thailand	80931	Yes	Yes	Yes			
3	Cambodia	2011	KT452799	III	Indian Subcontinent	V0907330-AC23	Yes	Yes	Yes	Yes	Yes	Yes
3	Fiji	1992	L11422	I	Southeast Asia/South Pacific	29472	Yes	Yes	Yes	Yes	Yes	
3	Indonesia	1978	KT452798	I	Southeast Asia/South Pacific	Sleman-1280-AC25	Yes	Yes	Yes	Yes	Yes	
3	Nicaragua	2009	HQ541806	III	Indian Subcontinent	BID-V4753	Yes	Yes	Yes	Yes	Yes	
3	Puerto Rico	1963	KT452800	IV	Americas	PRS-228762-AC27	Yes	Yes	Yes	Yes	Yes	
3	Puerto Rico	2006	EU529698	III	Indian Subcontinent	429965	Yes	Yes	Yes	Yes	Yes	
3	Vietnam	2006	EU660409	II	Thailand	BID-V1329	Yes	Yes	Yes	Yes	Yes	Yes
3	Vietnam	2007	FJ432743	II	Thailand	BID-V1817	Yes	Yes	Yes	Yes	Yes	
4	Brazil	2012	KT452794	II	Indonesia	BR-12	Yes	Yes	Yes			
4	Myanmar	2008	KT452793	I	Southeast Asia	81087	Yes	Yes				
4	Cambodia	2010	KF543272	I	Southeast Asia	U0811386	Yes	Yes	Yes	Yes	Yes	
4	Cambodia	2011	KT452802	I	Southeast Asia	V0624301-AC33	Yes	Yes	Yes	Yes	Yes	Yes
4	Dominica	1981	AF326573	II	Indonesia	814669-42A	Yes	Yes	Yes	Yes	Yes	Yes
4	Indonesia	1978	JN022608	II	Indonesia	S1228		Yes	Yes	Yes		
4	Indonesia	1973	KT452801	II	Indonesia	M30153-AC36	Yes	Yes	Yes	Yes	Yes	Yes
4	Malaysia	1973	JF262780	Sylvatic	Sylvatic	P73-1120	Yes	Yes	Yes		Yes	
4	Nicaragua	1999	KT452803	II	Indonesia	703	Yes	Yes	Yes			
4	Puerto Rico	1998	EU854297	II	Indonesia	347751		Yes	Yes	Yes	Yes	
4	Puerto Rico	1999	FJ882599	II	Indonesia	BID-V2446	Yes	Yes	Yes	Yes	Yes	Yes
4	Thailand	1985	AY780644	I	Southeast Asia	D85-052		Yes	Yes	Yes	Yes	

Table S1. Epidemiological and genetic information for the DENV panel. Viruses are labeled by genetic type, location and year of isolation, GenBank number, genotype (Holmes and Twiddy, as well as Rico-Hesse nomenclature), unique identifier, whether they were used to generate the monkey antisera, and whether they were titrated against each panel of antisera (*15*, *43*).

1.1.2. Phylogenetic analyses

Nucleotide sequences (n=47) for the envelope (E) protein gene were obtained from GenBank or sequenced by members of the Dengue Antigenic Cartography Consortium and easily aligned using MAFFT (http://www.ebi.ac.uk/Tools/msa/mafft/). In Fig. 1A, the phylogenetic relationships among these nucleotide sequences were estimated from 2 random starting trees using the maximum likelihood (ML) method available in the PhyML program (version 3.0; http://www.atgc-montpellier.fr/phyml/), assuming the general time reversible (GTR) nucleotide substitution model with four discrete gamma (Γ) categories of among-site rate variation and allowing for invariant sites (i.e. GTR+Γ_4+I model) as chosen by jModeltest2 (http://code.google.com/p/jmodeltest2/) (*44*, *45*). The ML tree topology was estimated using a combination of Nearest Neighbor Interchange (NNI) and Subtree Pruning and Regrafting (SPR) branch-swapping (*46*). Bootstrapping (1000 replicates) was used to assess the branch support for the ML tree of 2 random starting trees. Nodes with ≥75% agreement among trees are labeled.

Using the same method, an additional phylogenetic tree of the DENV panel within the context of a larger set of isolates (n=129) is shown in fig. S1.

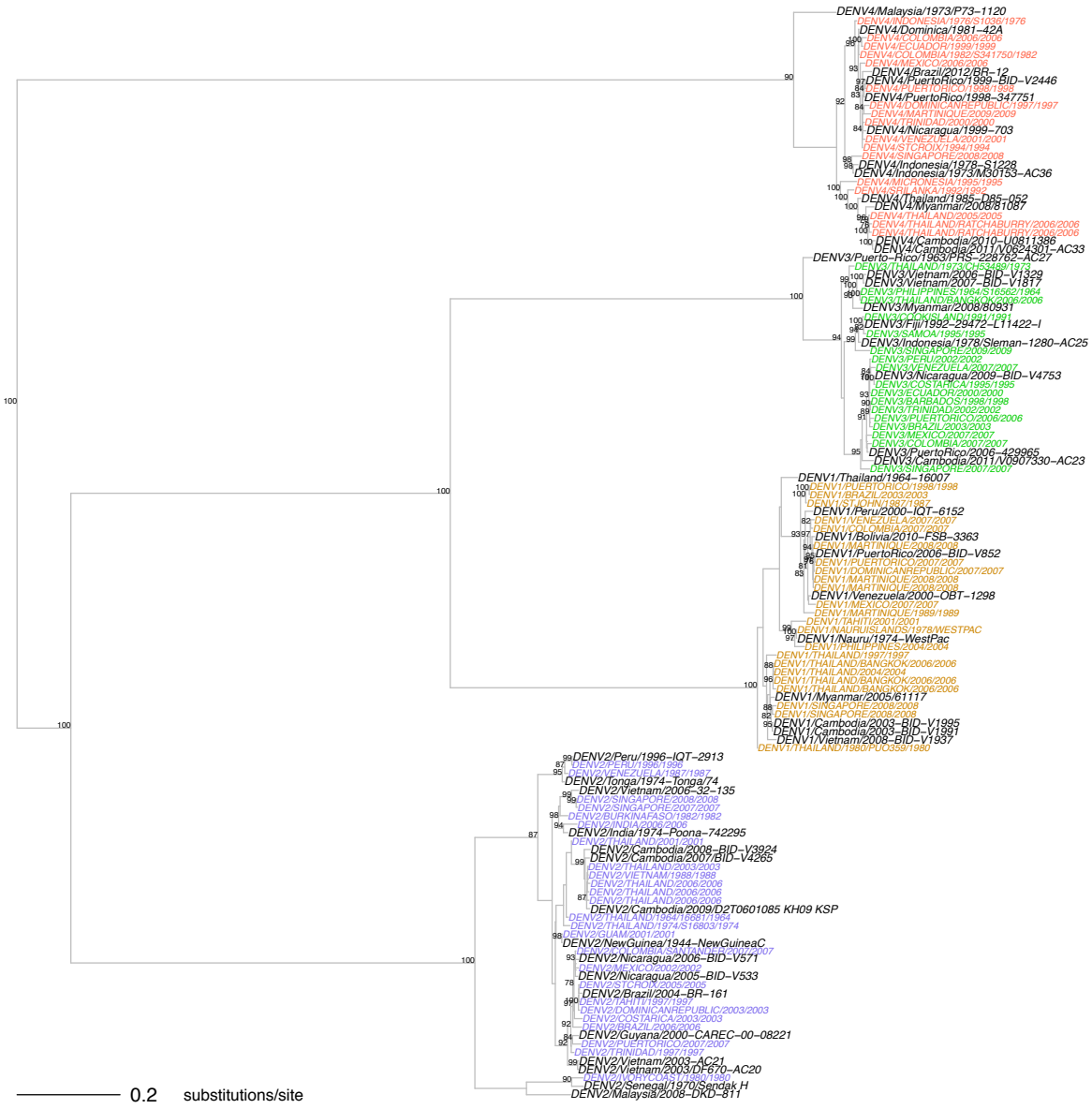

Fig. S1. A maximum likelihood phylogenetic tree of the DENV panel within the context of a larger set of isolates. E gene sequences for the large sample are colored by type (yellow=DENV1, blue=DENV2, green=DENV3, red=DENV4) and viruses included in the present study are shown in black. Viruses are labeled by type, location and year of isolation, and unique identifier.

1.1.3. Genetic maps

DENV E gene nucleotide sequences were converted to amino acid sequences, and the genetic distance between them was defined as the number of pairwise amino acid differences. The genetic map shown in Fig. 1B was made using cartography techniques, described below and in Smith *et al.* (*25*). Two additional genetic maps were made, for which differences were counted only for amino acids predicted to be exposed on the E monomer of a representative DENV2 (PDB ID: 10AN, defined as amino acids that had ≥50% of the atoms exposed), or those unlikely to be concealed on the monomers of representative DENV1, DENV2, and DENV3 (PDB IDs: 10AN, 1UZG, 4GSX, ≥20% atoms exposed) using GETAREA (http://curie.utmb.edu/getarea.html) (fig. S2) (*47*). The conclusions from these two additional genetic maps were the same as the interpretation of the genetic map of all positions: the distance within type is far less than the distances between types.

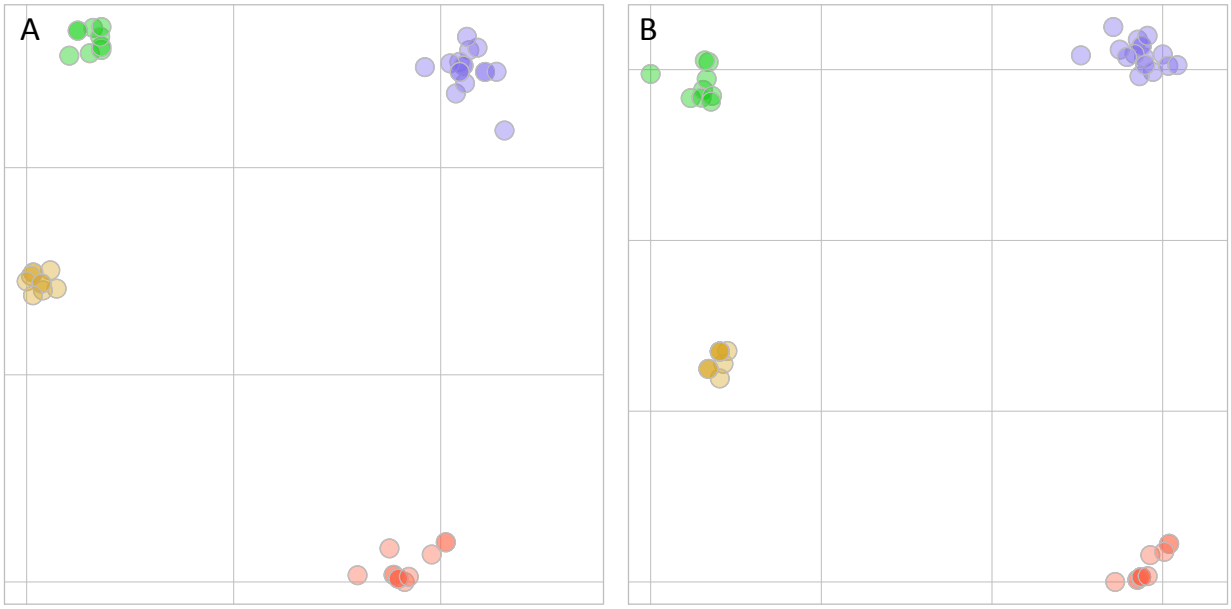

Fig. S2. Genetic maps of the DENV panel (n=47), but with distance between pairwise sequences measured for only subsets of E protein amino acid positions. (**A**) Only amino acid positions predicted to be exposed on the E monomer of a representative DENV2 virus. (**B**) The intersection of amino acids unlikely to be concealed within E monomers of representative DENV1, DENV2, and DENV3 isolates (*47*). Each grid-square side corresponds to 20 amino acid differences.

1.2. Sets of antisera

1.2.1. African green monkey antisera

A model animal, the African green monkey (*Chlorocebus sabaeus,* hereafter NHP*)*, was selected for the initial antigenic characterization. First, antigenic cartography necessitates the use of primary exposure antisera because an individual who has been infected multiple times with antigenically distinct viruses will likely show neutralization to each virus from a previous infection. If an antiserum from this individual is used to make an antigenic map, the viruses may appear antigenically similar to one another, although they do not share common antigenic properties (*14*).

Identifying individuals with a primary DENV exposure in endemic settings is challenging. To do so, researchers often employ criteria based on undetectable pre-infection neutralization, IgM/IgG ratio during acute infection, and post-infection neutralization primarily to a single DENV type (*48*). These methods are sufficient for most research on DENV neutralizing responses. However, it was essential to design our first experiment so that if unusual neutralizing responses were observed, such as similar cross-neutralization of homologous and heterologous DENV variants by a given antiserum, we could be certain that it was a result of a primary infection. When a monotypic response is a prerequisite for identifying primary infections, it may bias antigenic studies so that it is only possible to see viruses cluster as serotypes.

Second, to create a stable and informative antigenic map, we sought a panel of antisera raised against genetically diverse isolates to increase the likelihood of being able to detect antigenic differences among viruses. Below, we describe making antigenic maps with antisera from individuals inoculated with the same antigen as a comparison.

Third, we wished to use antisera drawn at the same time point after infection to control for variation among antisera that may arise from temporal changes in the immune responses. Epidemiological studies have found the period of cross-protection against clinical infections by heterologous types following first infection to be at minimum two months for individuals, and on average at the population level two years against symptomatic infection and 3.5 years against hospital infection (*6*, *29*, *49–52*). It is common for vaccine studies in non-human primates to challenge vaccine protection one to six months after infection (*53*, *54*).

There is no animal that serves as an ideal model for human DENV infection. However, the immune response mounted by non-human primates is believed to be antigenically relevant to human infection, and is widely used for dengue vaccine development and research (*35*).

Viruses for inoculation were chosen so that the panel of antisera would capture a wide range of genetic variation within each DENV type (table S1). Eighteen NHPs (juvenile and young adult, male and female, from St. Kitts) determined to be seronegative by immunofocus reduction neutralization test to dengue, West Nile, and yellow fever viruses (<1:10 $FRNT_{50}$ titer)

were included in the study. Seventeen NHPs were randomly assigned a virus inoculum and injected subcutaneously in the right and left arm each with 0.5 ml of $1*10^5$ immunofocus forming units/mL (ffu/mL) as determined using the DENV titration test described below. One NHP received a placebo inoculum of Leibovitz L-15 medium (Lonza, Walkersville, MD), and was otherwise treated the same as other NHPs. NHPs were monitored twice daily for mortality and morbidity. Blood samples were collected on days 1, 2, 3, 4, and 7 post-inoculation to detect viremia, and on day 30 (one-month) and day 149 (five-month) post-inoculation for use in neutralization tests. None of the NHPs were detected to be viremic at a limit of detection of 50 ffu/mL serum over the first week post-inoculation. Sera were extracted from the one, three, and five-month post-inoculation blood samples and stored at -70°C. This study followed the National Institutes of Health guidelines for the humane treatment of laboratory animals and was approved by the NIAID Animal Care and Use Committee. One NHP had very poor neutralizing responses at all three time points, and was excluded from antigenic analyses.

1.2.2. Human monovalent vaccine antisera

De-identified human immune sera previously collected from adults given the NIH monovalent DENV vaccines (ClinicalTrials.gov identifiers: NCT00473135 NCT00920517, NCT00831012, NCT00831012) were provided by Dr. Anna Durbin. The trials were performed under an investigational new drug application reviewed by the US Food and Drug Administration and approved by the Institutional Review Board at the University of Vermont and Johns Hopkins University. Informed consent was obtained in accordance federal and international regulations (21CFR50, ICHE6).

1.2.3. Human natural primary infection antisera

We assembled a panel of antisera from children naturally infected with dengue while enrolled in the Pediatric Dengue Cohort Study in Managua, Nicaragua (3,500 total children age 2-14 enrolled) (*55*). This study was approved by the Institutional Review Boards of the Nicaraguan Ministry of Health and the University of California, Berkeley. Parents or legal guardians of all subjects provided written informed consent, and subjects 6 years of age and older provided assent. Children who present to the study Health Center Sócrates Flores Vivas with fever are screened for dengue, and acute and convalescent (day 14-21) blood samples are collected from suspected dengue cases and undifferentiated febrile illnesses. A healthy annual blood sample is also collected from all participants, and paired annual samples are measured for anti-DENV antibody titers by inhibition ELISA.

Children with a four-fold seroconversion by inhibition ELISA were selected for further analysis of neutralizing titers using a flow-cytometry based assay on Raji-DC-SIGN cells using reporter virus particles (RVP) representing each of the four DENV types (*50*). Based on the RVP neutralization titers, we selected a panel of 20 antisera drawn in the year after each child's primary infection. Samples were selected only if the children had <10 titers to all four DENV types for all years they were enrolled in the study prior to their first infection, which ranged from one to three years. Five antisera were selected for each infecting type: the infecting type was identified by PCR or virus isolation for symptomatic infections, and by the highest of the four RVP neutralizing titers for inapparent infections. We selected a representative set of antisera for

each type that ranged from type-specific to cross-reactive, to avoid the traditional bias in post-infection screening for primary infection responses. For each type, we selected two type-specific antisera with higher neutralizing titers, one antiserum that was type-specific but had low neutralizing titers, and two antisera that had more cross-type reactive neutralizing responses. We did not consider whether the infection was symptomatic or inapparent.

We tested if older children, who were at risk of DENV infection longer, were consistently more cross-reactive, suggesting that they might not be true primary infections. We used the RVP neutralization titers to estimate the degree of cross-reactivity for each child as the ratio of the highest titer to any strain to the median of the four titers. There was no significant relationship (linear regression) between age at the time of infection and degree of cross-reactivity ($p=0.24$). There was also no significant relationship between age at infection and maximum titer ($p=0.95$).

We also tested how representative the neutralizing responses of the 20 children studied here were of the responses of children in the larger cohort. We compared the RVP titers of the 20 children to those of 71 additional primary infection antisera, and found that they did not significantly differ in degree of cross-reactivity ($p=0.24$) or maximum titer ($p=0.45$).

1.3. Neutralization assay experimental methods

1.3.1. Use of Aedes albopictus cell line

Viruses from infectious serum samples are more robustly amplified on mosquito cells than mammalian cells, and thus *Aedes albopictu*s (C6/36) cells are commonly used for virus isolation (*56*, *57*). Additionally, DENV isolates passaged multiple times in C6/36 cells accumulate amino acid substitutions more slowly than similar passage in human cells (*58*). C6/36 cells were chosen as the target cells for this experiment to eliminate the need to adapt viruses to a mammalian cell line and potentially introduce mutations that may alter antigenic properties.

1.3.2. DENV amplification in Aedes albopictus cells

Flasks with confluent C6/36 cells (*Aedes albopictus*, NIAID/Novavax MCB, passage ≤ 21) were inoculated with 0.5 mL virus stock and incubated for 4-6 days at 32°C. (Note: incubations were conducted under conditions of 5% CO_2 and 80% relative humidity at 32°C or 37°C.) For virus harvest, 1X SPG (Sucrose-Phosphate-Glutamate stabilizer, laboratory preparation) was added to flasks, fluid was centrifuged at 1000 g for 5 minutes, and supernatant was aliquoted and stored at -70°C.

1.3.3. Virus titer determination

The titer of each virus sample was determined with a DENV titration test (*26*). Virus samples were rapidly thawed at 37°C and diluted 1:10 in 0.1 mL diluent, made with OptiMEM GlutaMAX (Invitrogen, Carlsbad, CA), 2% fetal bovine serum (FBS, HyClone Laboratories, Logan, UT), 50 µg/mL gentamicin (Invitrogen), and 0.5% albumin (Bayer, Walkersville, MD). Eight 10-fold serial dilutions were prepared in duplicate in 96-well CoStar plates (Sigma-Aldrich, St. Louis, MO) and incubated at 37°C for 30 minutes. Virus dilutions (0.03 mL) were added in duplicate to 96-well plates of confluent C6/36 cells and incubated at 37°C for 1 hour. After incubation, 0.15 mL warmed overlay medium (37°C) was added, consisting of OptiMEM GlutaMAX, 1% methylcellulose (EMD Chemicals, Billerica, MA), 2% FBS, 2.5 µg/mL Amphotericin B (Quality Biological, Gaithersburg, MD), and 20 µg/mL Ciprofloxicin (Bayer). Plates were incubated at 32°C for 3-4 days. Wells were stained following the immunostaining protocol detailed below. Mean virus titer was measured in ffu/mL and estimated from the average of duplicate wells at the virus dilution at which approximately 10-60 immunofoci were present.

1.3.4. Antigenic characterization with the immunofocus reduction neutralization test

For each neutralization titration, NHP serum was rapidly thawed, diluted 1:10 in diluent (OptiMEM, 2% FBS, 50 µg/mL gentamicin, and 0.5% albumin), and heat inactivated in a water

bath at 56°C for 30 minutes. Twelve two-fold serial dilutions of antisera (1:10 to 1:20,480 with 0.04 mL per well) were prepared in 96-well plates. DENV samples were diluted to yield an expected count of 30-50 immunofoci per well, and 0.04 mL of the diluted virus samples were added to the serum dilutions. Although the dilution of the antiserum in the final virus-serum mixture ranges from 1:20 to 1:40,960, we report serum dilution prior to mixing with virus (1:10 to 1:20,480).

Plates were incubated for 30 minutes at 37°C. Aliquots of the serum-virus mixture (0.03 mL) were added in duplicate to 96-well plates of confluent C6/36 cells, and incubated for 1 hour at 37°C.

After incubation, 0.015 mL warmed overlay medium (OptiMEM GlutaMAX, 1% methylcellulose, 2% FBS, 2.5 µg/mL amphotericin B, 20 µg/mL ciprofloxicin, at 37°C) was added to wells, and plates were incubated for 3-4 days at 32°C.

1.3.5. Immunostaining protocol

Plates were removed from the incubator and overlay medium was discarded. Plates were washed twice with phosphate buffered saline (PBS buffer), and fixed at room temperature for 10 minutes with 0.1 mL of 90% methanol. Methanol was removed, and an antibody dilution buffer, made with 1X PBS and blocking agent 5% weight/volume non-fat dry milk, was added to wells and left for 10 minutes. Flavivirus mouse monoclonal antibody 4G2 (HB112 hybridoma from ATCC, Manassas, VA) was diluted 1:2000 in antibody dilution buffer and 0.1 mL was added to each well inoculated with DENV2, DENV3, and DENV4 as a primary antibody. Mouse monoclonal antibody 4G2 does not bind well to some DENV1 viruses: thus, a different antibody, mouse monoclonal HB114 (D3-2H2-9-21, ATTC) was used as a primary antibody for DENV1 viruses. Plates with the primary antibody solution were shaken gently at 37°C for 1 hour. Primary antibody solution was removed, and plates were washed twice with 0.18 mL antibody dilution blocking buffer. Peroxidase-labeled goat anti-mouse IgG (Kirkegaard & Perry Laboratories, KPL, Gaithersburg, MD) was diluted 1:3000 in antibody dilution buffer, 0.1 mL was added to each well, and plates were shaken gently at 37°C for 1 hour. The secondary antibody solution was removed, and plates were washed twice with PBS. Plates were allowed to dry for 10 minutes before adding 0.06 mL TrueBlue Peroxidase substrate (KPL), which was left on wells until immunofoci were clearly distinguishable (10-40 minutes). The TrueBlue substrate was then removed, and plates were scanned using the ImmunoSpot Analyzer (CTL, Shaker Heights, OH).

1.4. Immunofocus counting and neutralization titer estimation

1.4.1. Immunofocus counting method

We used R to analyze all immunofocus reduction neutralization test data (R Foundation for Statistical Computing, version 3.1.3). First, all images were trimmed with a circle of radius ½(image height)-40 pixels to exclude well edges, which often contain reflections, excess liquid, and other distortions that may interfere with the immunofocus counter. The saturation channel from each image was extracted using the rgb2hsv() function from the grDevices package for further analysis. Images were smoothed to reduce noise in the image with a gaussian blur using the gblur() function in the EBImage package. After blurring, the pixel data were transformed to increase the difference between background and immunofocus signal. This included squaring or cubing all pixel values, (images with paler, small immunofoci were squared while larger, darker immunofoci cubed), and multiplying that value by a constant, which ranged from 0.5 for images with darker background to 3 for those with lighter background. After the transformation, values >1 are set to 1, and all values <0 are set to 0. The function thresh() from the EBImage package was then used to threshold the data and identify immunofocus shapes, using a square filter of 30 by 30 pixels, and an offset between 0.08-0.12, manually determined depending on background and immunofocus intensity. All objects resulting from the thresholding step were slightly dilated using the dilate() function in EBImage with a disk radius of 11 pixels to ensure clusters of small objects were correctly counted as uniform immunofoci. The watershed() function with a tolerance of 3 was used to divide large distinct shapes that were only slightly overlapping. All remaining objects greater than 20 pixels in size were counted as immunofoci. As a validation, one well on each of the 1634 plates was checked by eye to ensure accurate counting of all objects as immunofoci.

We also tested for immunofocus overlap in our system. A virus with a high expected number of immunofocus forming units per well was serially diluted in two-fold and added to cells. The resulting immunofocus count declined by two-fold at each step, indicating there was not a problem with immunofocus overlap (fig. S3 and table S2). The watershed algorithm was also run on the immunofocus image data, and the immunofocus count still dropped by two-fold for each serial virus dilution.

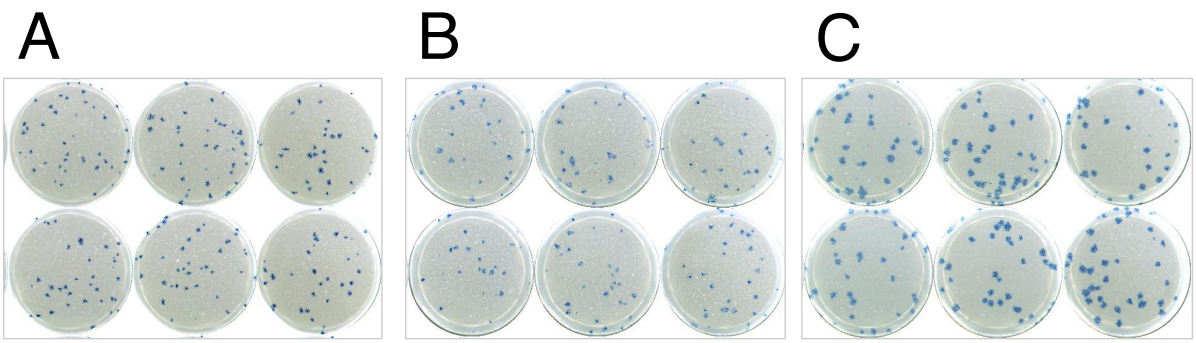

Fig. S3. Representative images of immunofoci for three virus stocks (A-C) used for immunofocus overlap analysis.

	Undiluted		1:2		1:4		1:8	
	Mean	SD	Mean	SD	Mean	SD	Mean	SD
Virus-1	63	7.1	29	4.7	18	4.8	6	2.8
Virus-1-watershed	66	9.3	31	5.0	18	5.0	6	2.7
Virus-2	56	4.8	35	4.3	20	5.8	8	2.4
Virus-2-watershed	59	5.9	35	4.4	19	6.2	9	2.7
Virus-3	97	5.5	53	4.9	31	2.5	19	5.0
Virus-3-watershed	111	11.3	56	4.4	33	3.5	19	4.9

Table S2. Three virus stocks (Virus 1-3) with high expected number of immunofocus forming units per well were prepared in four two-fold serial dilutions, ranging undiluted to 1:8. Mean and standard deviation for 6 duplicate wells are shown. Images of immunofoci were also counted with an added watershed segmentation ("-watershed") to separate touching objects in the image data.

1.4.2. $FRNT_{50}$ titer determination

Immunofocus count data were imported into R (R Foundation for Statistical Computing, version 2.15.2) for statistical analyses. The neutralization titer was defined as the reciprocal serum dilution at which 50% of the virus population was neutralized for each virus-serum pair relative to the average immunofocus count for wells in which there was no neutralization ($FRNT_{50}$). The number of immunofoci present in wells with no neutralization was estimated as the mean immunofocus count in wells with antiserum dilutions greater than 1:5,120 (6 wells per titration, ~120 wells per virus) for each tested virus. The neutralization titer was calculated using the drm() function in the drc package from a two-parameter (slope and intercept) logistic regression of the immunofocus counts for all 24 wells, and is reported as the reciprocal serum dilution. The raw neutralization titers for the one, three and five-month NHP, the monovalent vaccine, and natural infection antisera data sets are listed in tables S3-S7, respectively, (see additional excel files).

1.4.3. Positive and negative controls

Three control samples were titrated against each virus in each experiment. Viruses were repeatedly titrated (on average, 4.6 times) against a positive control: a DENV-positive infection antiserum. The average standard deviation of repeats across the DENV panel was 1.5-fold (SD: 1.3-fold). Two negative controls, NHP placebo antiserum and medium-only, were also included for each experiment. In 204 experiments, 87% of placebo-only titrations had titers <10, and 100% titers <20. When repeated, the numeric placebo values consistently dropped to <1:10. In 216/217 experiments, the medium-only titrations had titers of <10.

A control virus, DENV2/Vietnam/2003-AC21 and its homologous serum, were included when each virus was tested against a serum panel. In 81 independent experiments, the estimated titer had a mean of 1:341 and standard deviation of 2.1-fold.

1.5. Antigenic cartography methods

1.5.1. Brief description of antigenic cartography

A full description of the technique of antigenic cartography has been published previously (software available at https://github.com/acorg/lispmds, web-based software available at https://albertine.antigenic-cartography.org:1168) (*25*). Briefly, each neutralization titer N_{ij} was transformed into a table antigenic distance D_{ij} between virus i and antiserum j by calculating the difference between the titer for the virus *best* neutralized by each antiserum j, defined as b_j, and the measured titer for each virus N_{ij} against that antiserum: $D_{ij}=log_2(b_j)-log_2(N_{ij})$. (Notably, antigenic cartography does not assume that the highest antiserum titer b_j will be against the virus used to generate that antiserum. Sensitivity analyses for defining b_j are described in section 1.5.7 below.) To find the map distances, represented by the Euclidean distance d_{ij} between each virus i and antiserum j, the differences between the map and table distances were minimized, as defined by the error function $E=\sum_{ij}e(D_{ij},d_{ij})$. The error of a serum-virus pair was defined as $e(D_{ij},d_{ij})=(D_{ij}-d_{ij})^2$ when the neutralization titer was numeric (within the limit of detection of the neutralization test, which ranged from 1:10 to 1:20,480). The error was defined as $e(D_{ij},d_{ij})=(D_{ij}-1-d_{ij})^2\ (1/1+e^{-10(Dij-1-dij)})$ for threshold titers (below the limit of detection, <1:10), so that the titer contributed to the stress only if the map distance was less than the minimum specified target distance $(d_{ij} < D_{ij}-1)$.

To identify the antigenic map for which the distances between viruses and antisera most closely matched the table distances, viruses and antisera were assigned random starting coordinates and the error function was minimized using the conjugate gradient optimization method. Five thousand independent optimizations were conducted to increase the likelihood of finding a good minimum. The observed minimum error map is shown on a grid in which each square side corresponds to a two-fold antiserum dilution, or one antigenic unit (AU), in any direction, on the antigenic map. Thus, two grid square sides are a four-fold antiserum dilution, three grid square sides are an eight-fold antiserum dilution, etc.

1.5.2. Error lines and goodness-of-fit

Error lines represent the agreement between each measured neutralization titer and the corresponding map distance. For each titration, error lines show the difference between the table distance and the map distance, with half of the difference in error drawn as a line from the virus, and half from the antiserum. Thus, the distance between the ends of the lines is the map distance expected if the neutralization titer were fit exactly. Red lines show the amount by which the table distance exceeded the map distance, and blue lines the amount by which the map distance exceeded the table distance. Overall, all maps had low error. The error lines on each map are typically short and well distributed around each point (fig. S4).

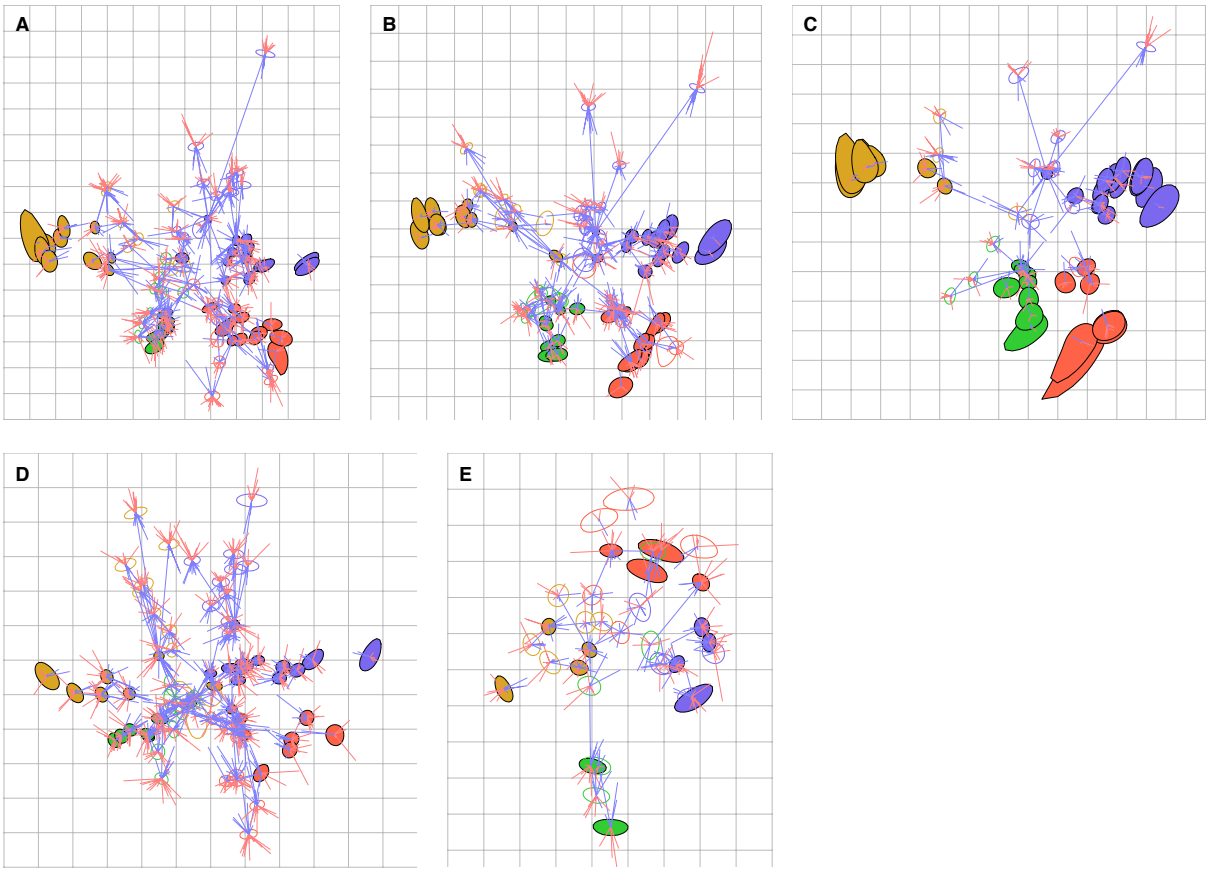

Fig. S4. Antigenic maps of the one-month NHP antisera (**A**), three-month NHP antisera (**B**) and five-month NHP antisera (**C**), human monovalent vaccine antisera (**D**) and human natural infection antisera (**E**) with error lines, which provide a quantitative and visual tool for assessing map fit. The distance between the ends of error lines corresponds to the measured titer: red lines indicate by how much the map distance exceeded the measured titer, and the blue lines by how much the measured titer exceeded the map distance.

Of note, two NHPs infected with DENV2 isolates had very high titers to DENV2/Vietnam/2003-AC21, and these titers were poorly fit in the NHP maps. These high

titers were repeatable, with similar patterns observed for antisera drawn at one, three and five months post-infection. When these titers were excluded in making the antigenic map, these two antisera clustered closer to the other DENV2 antisera (fig. S5). There are some differences in the positions of viruses (visualized as arrows pointing to the position of viruses and antisera when this titer is excluded), mostly for the most peripheral DENV1 isolates and some DENV4 isolates. Because the titers were observed in multiple experiments, we expect that they are real, and although they do not 'fit' as well with the data set as a whole, they are included in the remaining analyses.

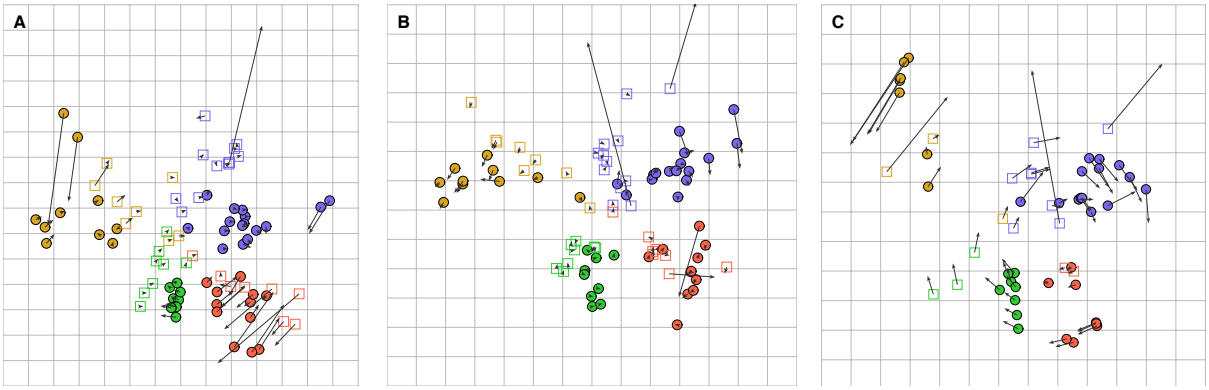

Fig. S5. The one (**A**), three (**B**) and five (**C**) month NHP maps with arrows pointing to the position of all antisera and viruses when the neutralization titers for two NHPs against DENV2/Vietnam/2003-AC21 are excluded.

The NHP inoculated with DENV1/Thailand/1964-16007 had almost no neutralizing titers at one, three and five months. It was exclude from the maps of all three data sets, because could not be coordinated (few numeric titers). One virus, DENV1-2003/Cambodia/ GQ868619 was excluded from the five-month map because it could not be coordinated (no numeric titers).

We also directly measured the disagreement between table distance and map distance (Fig. S6). Numeric titers (purple circles) were linearly related to their estimated map distances, with slopes ranging from 0.82-1.10 and intercepts from 0.73-0.88 (table S8) (the light black line represents the linear regression of the data, and the dark black line a local regression). Table distances for threshold titers (cyan open circles) were well-fitted, as most map distances were larger than the specified target distance (above the dotted black line showing 1:1 correspondence between table and map distances). When both numeric and threshold titers were considered, 8-11% of map distances for the NHP and monovalent vaccine maps exceeded measured titers by more than two-fold, and only 1-2% by more than four-fold. For the natural infection human map, 23% of map distances exceed measured titers by more than two-fold, but only 3% exceeded measured titers by more than a four-fold.

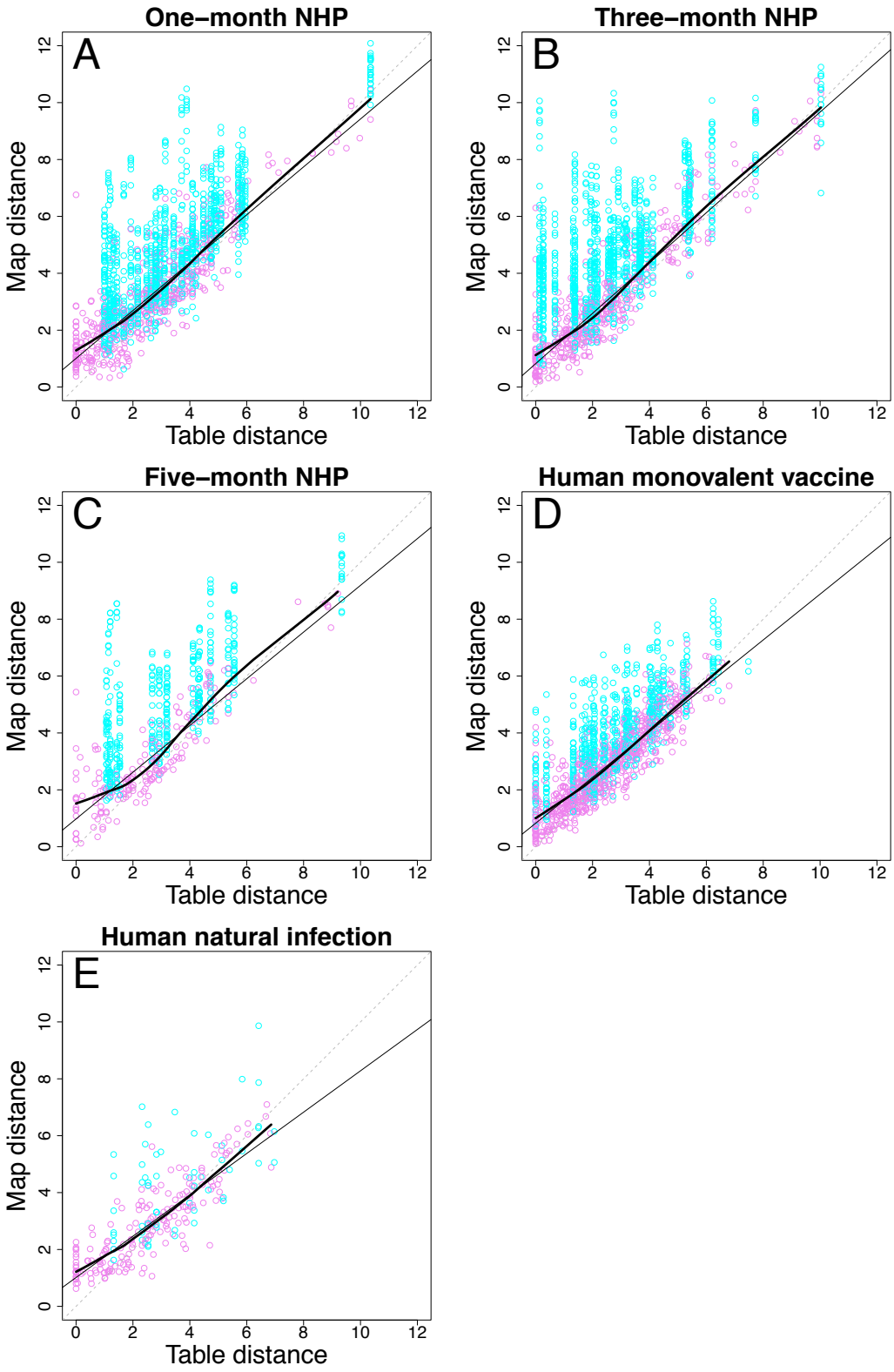

Fig. S6. Table distances plotted against map distances for the antigenic maps of the one-month NHP antisera (**A**), three-month NHP antisera (**B**), five-month NHP antisera (**C**), human monovalent vaccine

antisera (**D**) and human natural infection antisera (**E**). Table distances are derived directly from the numeric titers with the following equation: $\log_2(b_j)$-$\log_2(N_{ij})$, where b_j is the definition of zero antigenic distance (here, without any b_j adjustment) and N_{ij} is the measured neutralization titer. Linear regression (black solid line), loess (thick black curved line, span=0.75, first degree polynomial), and a perfect fit line (dotted line) are shown. Regression parameters are listed in table S8. Numeric titers (titers between 1:10 and 20,480) are colored pink, and threshold titers (<1:10) are colored cyan. Threshold titers are well fit so long as the map distance is equal or greater than the table distance (above the dotted line).

Linear regression of numeric table and map distances					**All table and map distances**	
	Slope	Intercept	R.S.E.	Adj. r^2	>Two-fold error	>Four-fold error
One-month NHP	0.84	1.01	0.89	0.77	11%	2%
Three-month NHP	0.88	0.82	0.8	0.85	8%	1%
Five-month NHP	0.82	0.98	0.84	0.77	8%	2%
Human monovalent vaccine	0.81	0.83	0.65	0.78	9%	1%
Human natural infection	0.73	1.01	0.73	0.75	23%	3%

Table S8. Goodness of fit of neutralization titers (table distances) by antigenic maps (map distances). The parameters that correspond to perfect fit of the numeric neutralization titers as a map distances were: one for slope and adjusted R^2, zero for intercept and residual standard error. The percent of titers fit with greater than two-fold or four-fold error was included to incorporate the goodness of fit of numeric and threshold titers simultaneously.

1.5.3. Coordination confidence

Coordination confidence areas (shapes on the antigenic map) indicate the amount of information in the data set on where to position each virus or antiserum relative to all other points (fig. S4). Larger shapes indicate that there is less information on where the virus or antiserum should be positioned. Round shapes have information on position from all directions, while long shapes are poorly coordinated in the direction in which they are longest. As expected, viruses and antisera in the middle of the antigenic maps are generally better coordinated (smaller, rounder shapes) than those on the periphery, as the former typically have more measurable titers, and hence more constraints to precisely position them.

Coordination confidence areas are constructed by freezing the positions of all but one point (virus or antiserum) on the map and allowing that point to move on spokes radiating out from the estimated map coordinates at 10° intervals until the total map error is increased by a predefined amount. An increase in total map error of 0.5, which is approximately the mean error contribution of each neutralization titration, was used for viruses and antisera all figures. The coordination confidence area for each virus and antiserum is interpolated from the position on each spoke where the specified error difference was observed.

Fig. S7 shows antigenic maps colored to indicate the degree to which viruses were neutralized by the panel of antisera. This is shown in three ways for the three-month NHP map. Each virus was colored by: 1) the mean of only numeric neutralization titers, 2) the mean of all titers, with titers <1:10 included as 1:5 titers, and 3) the number of measured titers that were >1:10. Yellow indicates low neutralizing responses, while red indicates strong responses. The

number of numeric titers is most strongly related to the antigenic position: viruses neutralized by more antisera were most centrally located on both maps. Both mean numeric titer and mean of all titers showed less correspondence with the antigenic position. Because the number of titers >1:10 was most strongly correlated with antigenic position, we only show this map for the one-month NHP map, five-month NHP, human monovalent vaccine map and natural infection map.

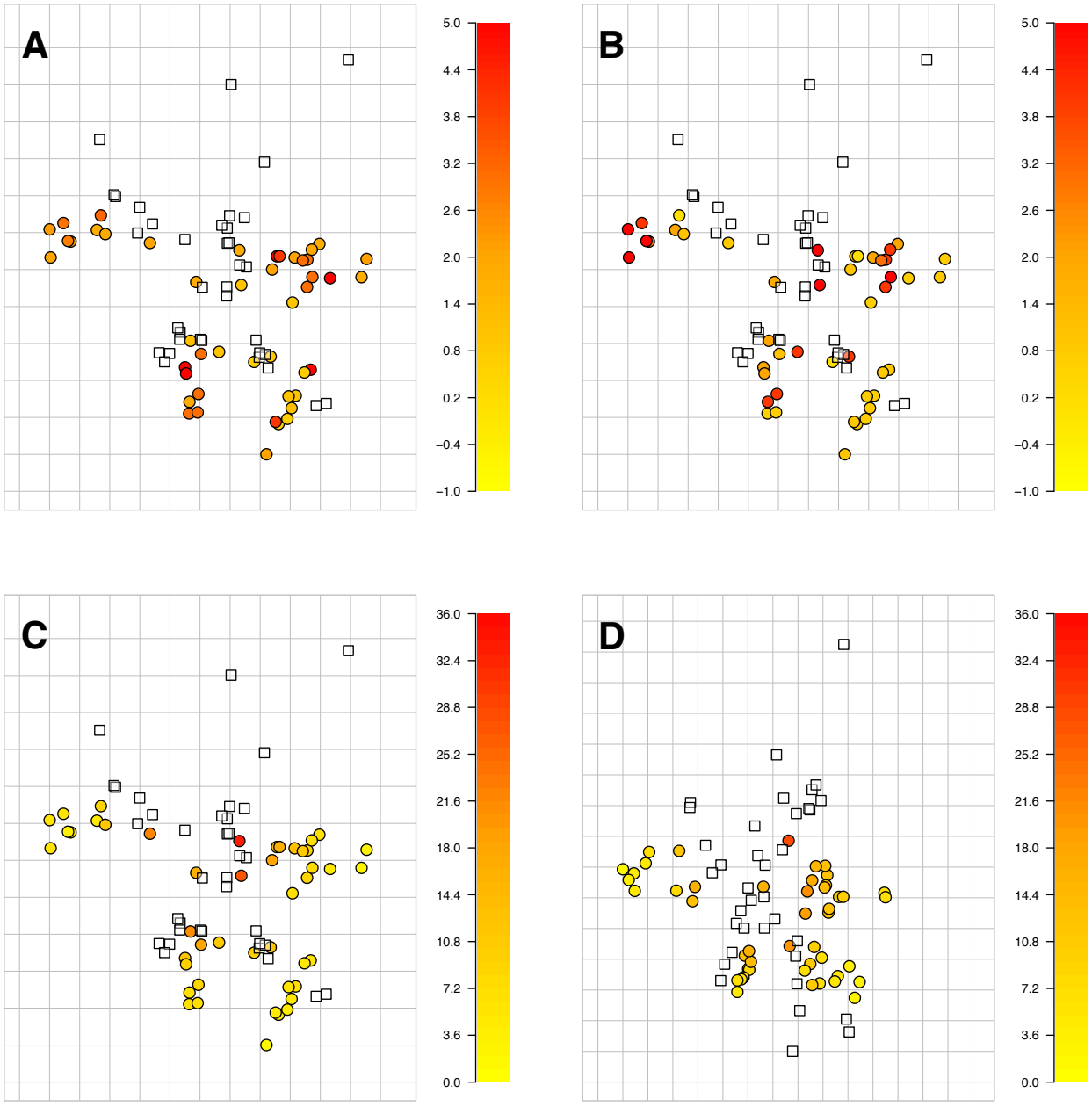

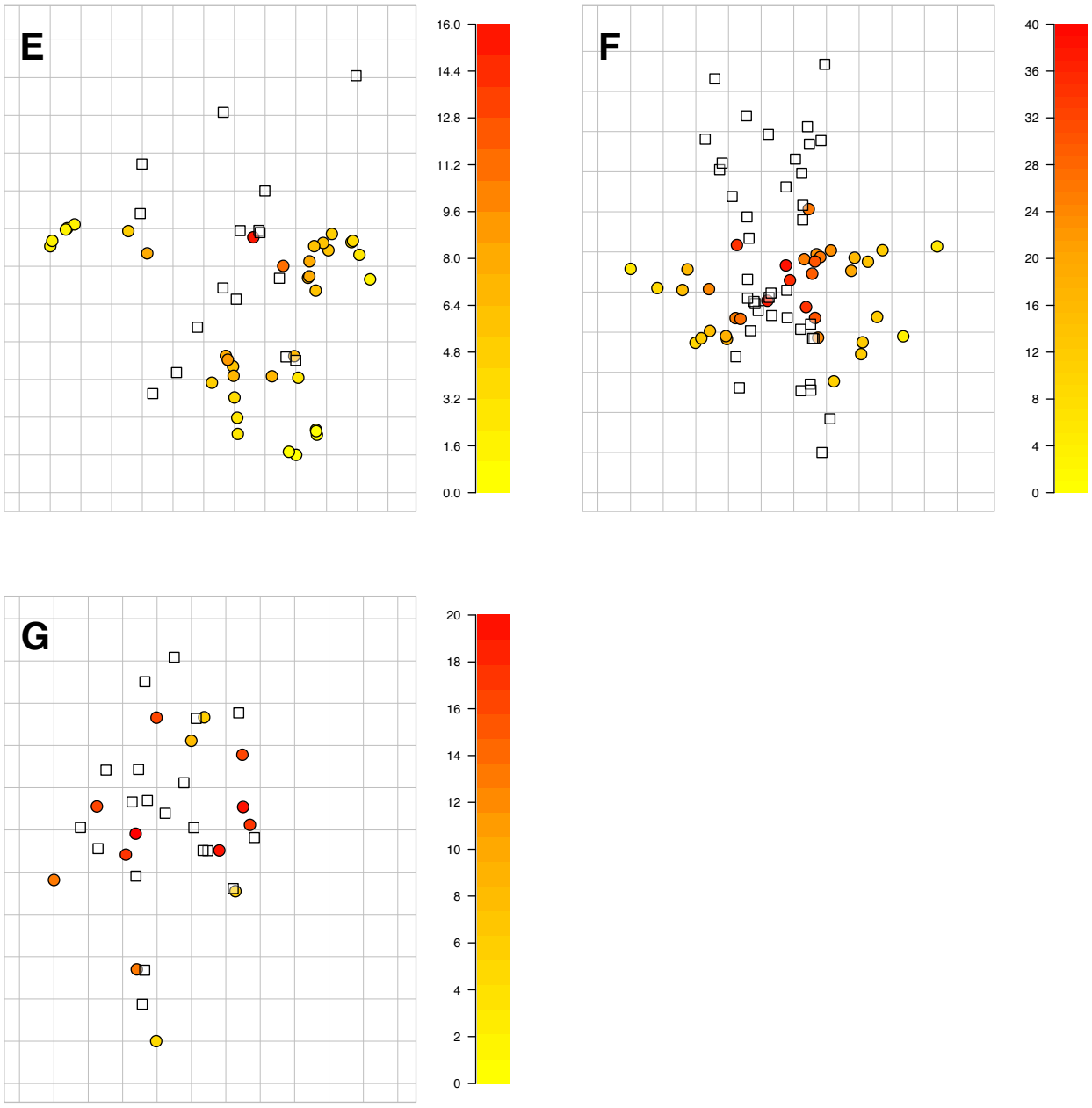

Fig. S7. Antigenic maps with each virus colored according to its degree of neutralization by the respective panel of antisera. Virus on the three-month NHP map are colored by the geometric mean of neutralization titers that were numeric (>1:10) (**A**), mean of all titers measured for that virus (<1:10 estimated as 1:5) (**B**), or by the number of antisera that neutralized the virus to at least a titer of 1:10 (**C**). One-month NHP (**D**), five-month NHP (**E**), human monovalent vaccine (**F**) and human natural infection maps (**G**) are colored by the number of titers. Geometric mean titers are estimated as the $\log_2$(titer/10), and range from <1:10 (-1, yellow) to 1:320 (5, red). The number of titers, ranging from 1 to the number of antisera in the set (from 16-40, depending on the data set), is also colored from yellow to red.

1.5.4. Sensitivity testing of FRNT neutralization titer values

One of the benefits of using an immunofocus assay rather than an HI assay is that it allows the calculation of full sigmoidal neutralization curves, which makes it possible to create antigenic maps with values other than the simple curve inflection point (corresponding to the $FRNT_{50}$ titer). With this approach, we tested if estimating a neutralization titer at alternative levels of neutralizing activity modified the clustering of viruses in relation to the classically described serotypes.

First, we used a lower criterion for neutralization, corresponding to a 40% reduction in neutralization, or $FRNT_{40}$ (fig. S8). The $FRNT_{40}$ increased the number of numeric titers in the data set, as some values that had previously been <1:10 values became numeric titers. However, use of the $FRNT_{40}$ also increased the value of all numeric titers. On the antigenic maps using $FRNT_{40}$ titers, the viruses centrally located on the antigenic maps overall moved slightly outward, while those that were already peripheral moved more toward the periphery. A few DENV1 and DENV4 isolates moved toward the center. Overall, the antigenic space occupied by each DENV cluster increased, but the distance between types remained the similar. The one-month NHP map and the human natural infection map had the most movement of viruses, mostly drawing the clusters closer together.

We also increased the criterion for neutralization and made antigenic maps using $FRNT_{60}$ titers (fig. S8). For the one and three-month NHP maps as well as the monovalent vaccine map, there are few shifts in virus position, and the largest changes were again observed for DENV1 and DENV4 viruses. The five-month NHP map has little resemblance to map in Fig. 4, with the DENV3 and DENV4 clusters switching position. The $FRNT_{50}$ titers in the five-month data set were already relatively low, and increasing the criterion for neutralization may have made it difficult to coordinate the viruses.

An additional sensitivity test determined the effect of interpolating neutralization titers below the assay limit of detection to a titer of 1:5 (fig. S8), increasing the number of numeric titers in the data set for titrations that were just below the limit of detection. Most isolates changed very little, except for a few shifts for DENV1 and DENV4 isolates. For the NHP maps and monovalent vaccine maps, this may be because some of the DENV1 and DENV4 infection antisera were just below the assay limit of detection, and so using the lower criterion for neutralization provided more information for positioning of viruses. There are a few larger shifts for DENV4 viruses in the human monovalent vaccine map and human natural infection maps.

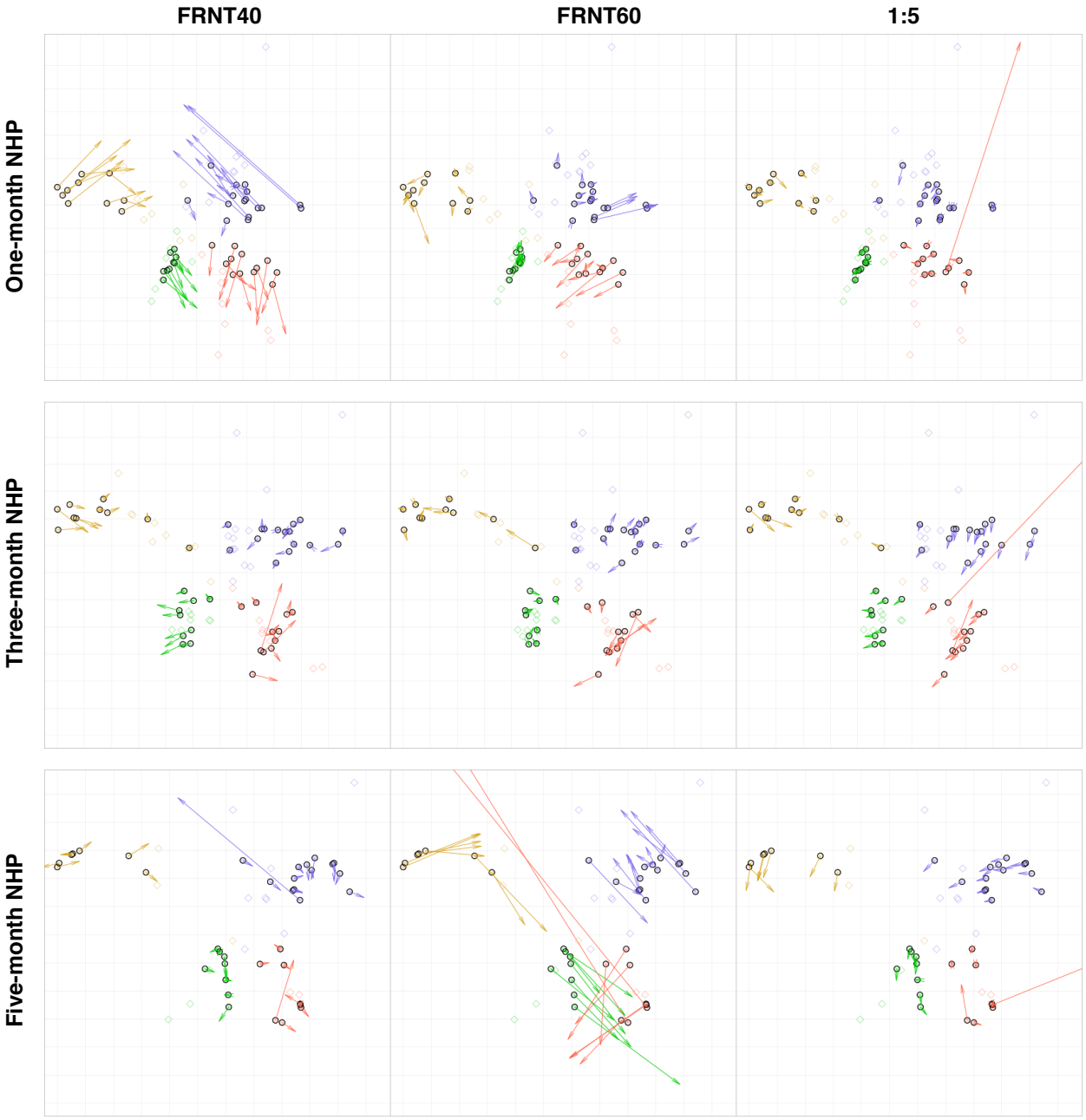
FRNT40
FRNT60
1:5
One-month NHP
Three-month NHP
Five-month NHP

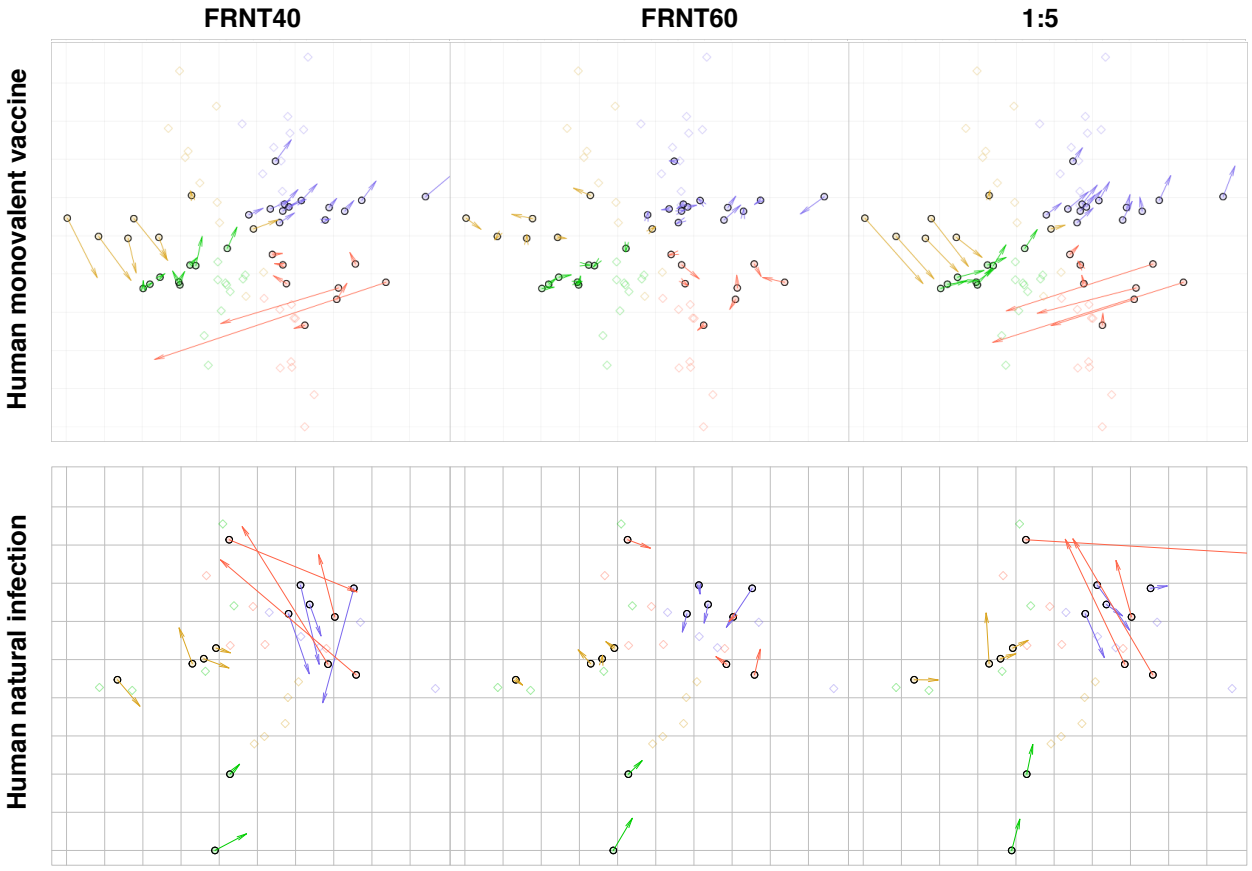

Fig. S8. Sensitivity analyses of the antigenic maps of one-month NHP antisera (**A**), three-month NHP antisera (**B**), five-month NHP antisera (**C**), human monovalent vaccine antisera (**D**) and human natural infection antisera (**E**). Maps were made using $PRNT_{40}$ titers (**left**), $PRNT_{60}$ titers (**center**), and $PRNT_{50}$ titers including estimation of values between 1:5-1:10 (**right**). The maps presented in the main manuscript are shown for all figures, with arrows pointing to position of the viruses and antisera in the sensitivity analysis.

1.5.5. Sensitivity testing of placebo and poorly neutralizing antisera

To test the effect of low-level neutralizing antisera on the coordination of viruses, we tested the effect of including the placebo antiserum, which showed low neutralizing activity against a few isolates in each data set. Because the placebo antiserum used in the monovalent vaccine antisera data set had the most titers >1:10, we tested if including the placebo antiserum altered the antigenic map. The placebo antiserum was positioned in the center of the antigenic map (cyan shape) and did not notably affect the positions of viruses or antisera on the antigenic map position (fig. S9).

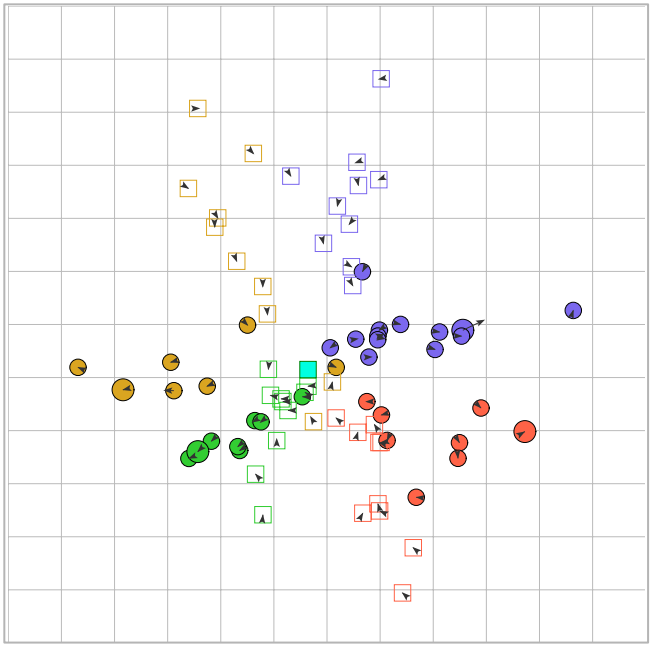

Fig. S9. The human monovalent vaccine antigenic map, with a placebo antiserum included (cyan square). Arrows point to the position of viruses and antisera on the map without the placebo antiserum included.

A few NHPs mounted poor neutralizing responses to DENV. Removal of these antisera had minimal effect on the positions of viruses or other sera on the antigenic map.

1.5.6. Dimensionality and cross-validation

Antigenic maps for all data sets were constructed in two, three, four and five dimensions (2D-5D) and compared for differences in error. In all cases, large reductions in the minimum observed error occurred between maps made in 2D and 3D, but modest reductions above 3D (table S9). The error calculations indicate that little was gained by fitting the neutralization tables in more than 3D, and thus testing for optimal antigenic maps was conducted in 2D and 3D.

To determine the number of dimensions that provided the best fit of the data set without over-fitting the data, we performed cross-validation experiments. One hundred antigenic maps were made in 2D and 3D, each from a random sample of 90% of titers. Neutralization titers were sampled from a data set for which each virus and antiserum had at least four numeric (>1:10) titers, so all could be coordinated in 3D. These maps were then used to predict the excluded 10% of titers (25 optimizations were conducted per trial). Considering both numeric and threshold titers, the one and three-month NHP maps have low cross-validation error, with a mean prediction error at one month of 0.54 and 0.52 in 2D and 3D, respectively, and 0.51 and 0.53 for three-month antisera in 2D and 3D, respectively (table S9). The prediction error was only slightly higher for the monovalent vaccine map. Overall, the differences between 2D and 3D across these data sets were small. The prediction error was slightly higher for the five-month NHP and natural infection maps, with greater difference between 2D and 3D. However, in all cases, the 2D map actually had slightly better correlation between measured and predicted titers

than the corresponding 3D maps (correlations ranged from 0.70-0.92). Because there were minimal differences between maps made in 2D and 3D, and 2D and 3D experiments performed similarly in cross-validation experiments, we present the 2D map as the main antigenic maps in the manuscript.

Dimensionality analyses

Percent reduction in stress	2D to 3D	3D to 4D	4D to 5D
One-month NHP	30%	13%	4%
Three-month NHP	19%	7%	3%
Five-month NHP	21%	3%	1%
Human monovalent vaccine	25%	13%	3%
Human natural infection	21%	4%	0%

Cross-validation analyses

One-month NHP map
44/47 viruses, 35/36 antisera

	2D	3D
Mean prediction error	0.54	0.52
Standard error	1.01	0.85
Correlation	0.90	0.88

Three-month NHP map
43/46 viruses, 30/36 antisera

	2D	3D
Mean prediction error	0.51	0.53
Standard error	0.93	0.86
Correlation	0.92	0.89

Five-month NHP map
22/37 viruses, 16/16 antisera

	2D	3D
Mean prediction error	0.83	0.86
Standard error	1.18	1.17
Correlation	0.90	0.85

Human monovalent vaccine map
36/36 viruses, 39/40 antisera

	2D	3D
Mean prediction error	0.61	0.62
Standard error	0.79	0.76
Correlation	0.91	0.85

Human natural infection map
14/14 viruses, 20/20 antisera

	2D	3D
Mean prediction error	1.23	1.14
Standard error	1.23	1.06
Correlation	0.70	0.68

Table S9. Dimensionality analyses of the antigenic maps. The percent reduction in error for each added dimension and comparison of cross-validation experiments are shown.

However, for visual comparison, we show the three-month NHP map in 3D. Similar to what was observed in 2D, DENV types in 3D formed diffuse clusters, but the four types were oriented as a tetrahedron (fig. S10). DENV1 and DENV4 were drawn slightly closer to one another, and DENV3 rotated away from DENV1 and DENV4 as compared to the 2D map. The structure within each type is mostly preserved, with viruses in the 3D map projecting consistently onto the 2D plane. A few DENV2 isolates project away from the DENV2 cluster and are pulled closer to the DENV1 and DENV4 clusters.

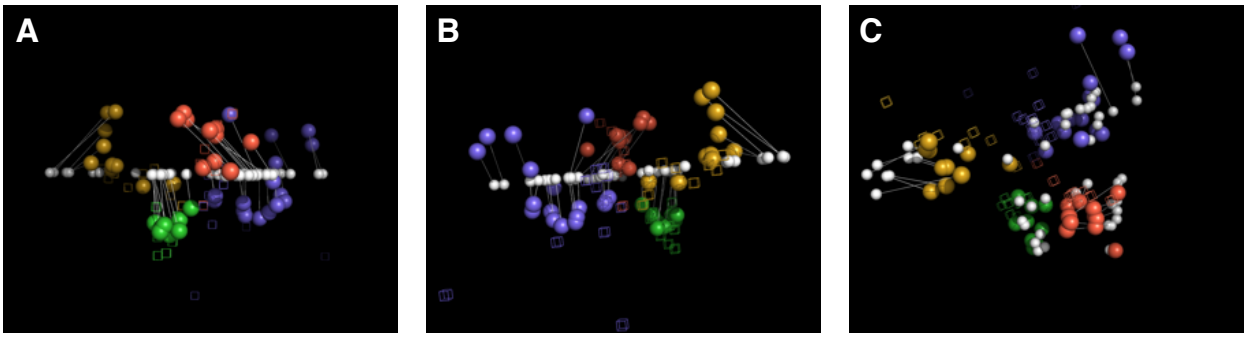

Fig. S10. Comparison of antigenic maps made in 2D and 3D of three-month NHP data set. The antigenic distance in 3D between each virus (colored spheres) and antiserum (open cubes, colored according to the infecting type) represents the measured neutralization titer, and like with the 2D map, each antigenic unit of distance (equivalent to one grid-cube side) is a two-fold difference in neutralization titer measurable in any direction. The corresponding viruses on the 2D antigenic map are shown as white spheres, with lines drawn between the corresponding viruses in the 2D and 3D locations. (**A-C**) show projections of the three-month map from different angles.

1.5.7. Optimizing column bases

To accurately infer antigenic distance in an antigenic map, the relationship between table distances D_{ij} and map distances d_{ij} must be linear, with a regression slope close to one and intercept close to zero. The degree to which the antigenic map meets this criterion may depend on the definition of zero antigenic distance on the map, b_j (or the 'column basis'), used for each antiserum. Using current antigenic cartography methods, there is no ideal tool for determining the optimal value of b_j for each antiserum.

For influenza antigenic cartography, the highest observed titer for each antiserum sets the value for zero antigenic distance, unless no values are at or above a dilution of 1:1280, in which case b_j is set to 1:1280. This approach works well for influenza, but is not suitable for many other pathogens, including DENVs, as many antisera have titers far below 1:1280 and there is no reason to assume each serum should be capable binding with such titers. Because the value of b_j can affect both the positions of viruses and antisera, we conducted sensitivity analyses to determine how maps were affected by different methods of setting the value of b_j. One disadvantage with all these approaches is that maps may be optimizing toward a 'degenerate' state, where distances are best satisfied by simply increasing the value of b_j so that no viruses in

the data set have titers close to zero antigenic distance and thus all viruses are pushed far away from the antisera. This can reduce the ability of the antisera to coordinate the viruses, and produce an uninformative geometric interpretation of the data.

For Figs. 2-4, the value of b_j was set to the maximum titer for each serum, what we here call "unadjusted column basis". We compare these maps to maps for which we adjusted the value for b_j for each antiserum (table S10). This adjustment was performed as follows: we started with the antigenic map with b_j set to the maximum titer for each serum. We then identified the value of b_j for each serum individually, with all other points frozen, that most reduced map error. We then remade the antigenic map with all the new b_j values. This constituted "one-iteration" of the column adjustment. We also repeated this iteration process until the subsequent iteration no longer reduced the map error, reaching a "converged" column adjustment. Each map required a different number of iterations before reaching convergence.

	Linear regression of numeric table and map distances				***All table and map distances***		
	Slope	Intercept	R.S.E.	Adj. r^2	>Two-fold error	>Four-fold error	*min bj*
One iteration bj adjustment							
One-month NHP	0.8	1.05	0.8	0.76	9%	1%	
Three-month NHP	0.89	0.74	0.72	0.84	6%	1%	
Five-month NHP	0.87	0.73	0.7	0.83	4%	1%	
Human monovalent vaccine	0.78	0.78	0.6	0.74	8%	1%	
Human natural infection	0.8	0.77	0.73	0.77	14%	1%	
bj until convergence							
One-month NHP	0.78	1.07	0.77	0.68	8%	1%	
Three-month NHP	0.88	0.74	0.7	0.81	5%	1%	
Five-month NHP	0.87	0.7	0.68	0.8	4%	1%	
Human monovalent vaccine	0.73	0.84	0.58	0.65	7%	1%	
Human natural infection	0.84	0.68	0.75	0.8	15%	2%	
640 min bj							
One-month NHP	0.81	1.09	0.86	0.74	11%	1%	
Three-month NHP	0.91	0.74	0.79	0.83	7%	1%	
Five-month NHP	0.85	0.86	0.77	0.77	5%	1%	
Human monovalent vaccine	0.8	0.86	0.64	0.73	8%	1%	
Human natural infection	0.73	1.01	0.74	0.74	23%	3%	
Antigenic maps of published data sets							
One-year monkey (Russell and Nisalak (1967)	0.92	0.75	0.58	0.88	9%	1%	max titer
Late-convalescent traveler (Messer *et al.* 2012)	0.86	0.55	0.69	0.84	19%	1%	max titer
Human monovalent vaccine (Durbin *et al.* 2013)	0.78	1.03	0.76	0.75	17%	2%	≥1,280
Human monovalent vaccine (Vasilakis *et al.* 2008)	0.81	0.53	0.64	0.71	6%	0%	≥320
Peruvian epidemic (Kochel *et al.* 2002)	0.84	1.08	1.04	0.82	37%	7%	≥20,480

Table S10. Goodness of fit of neutralization titers (table distances) by antigenic maps (map distances) made with adjusted column bases (b_j values), including a one iteration column adjust, converged column adjust, and minimum column basis set to 640. The parameters that correspond to perfect fit of the numeric neutralization titers as a map distances were: one for slope and adjusted R^2, zero for intercept and residual standard error. The percent of titers fit as greater than two-fold or four-fold error was included to incorporate the goodness of fit of numeric and threshold titers simultaneously. We also show the results of column basis testing for the antigenic maps of published data sets, and which minimum column basis allowed the best fit of each dataset.

We also investigated if a minimum value for b_j applied across all antisera for each map improved the fit of the data, using a similar approach to that used for influenza antigenic maps. We tested a range of minimum b_j values for each DENV data set, ranging from b_j defined at 1:80 to 1:2,560 (fig. S11). The b_j value that provided the best fit of table distances was selected for further analyses, which for all five maps was at a titer of 1:640 (table S10). Although the maps with b_j set to a minimum of 1:640 had lower error than the unadjusted column basis maps, the minimum b_j maps performed slightly worse in cross-validation experiments (data not shown), and thus were studied only as a sensitivity analysis, and not as the primary antigenic map. Further, the unadjusted maps, although slightly higher error, fit table distances as map distances without strong bias across the map (slopes were close to one and intercepts close to zero for all maps) (table S8 and fig. S6).

We also tested if a minimum value of b_j improved the fit of antigenic maps of previously published data (the values for b_j used to fit each data set are included in table S10). Two data sets (Messer *et al.* 2012 and Russell and Nisalak 1967) were only slightly better fit with a minimum b_j value above the maximum observed titer, and overall fit table distances as map distances with minimal bias even without adjusting the column bases. The antigenic maps of these data sets are shown without adjustment. The other three data sets had strong bias in map distances without a minimum column basis: the relationship between table and map distances greatly deviated slope of one and intercept of zero. Thus for these data sets, the b_j value that produced maps with the lowest error were selected for these data sets.

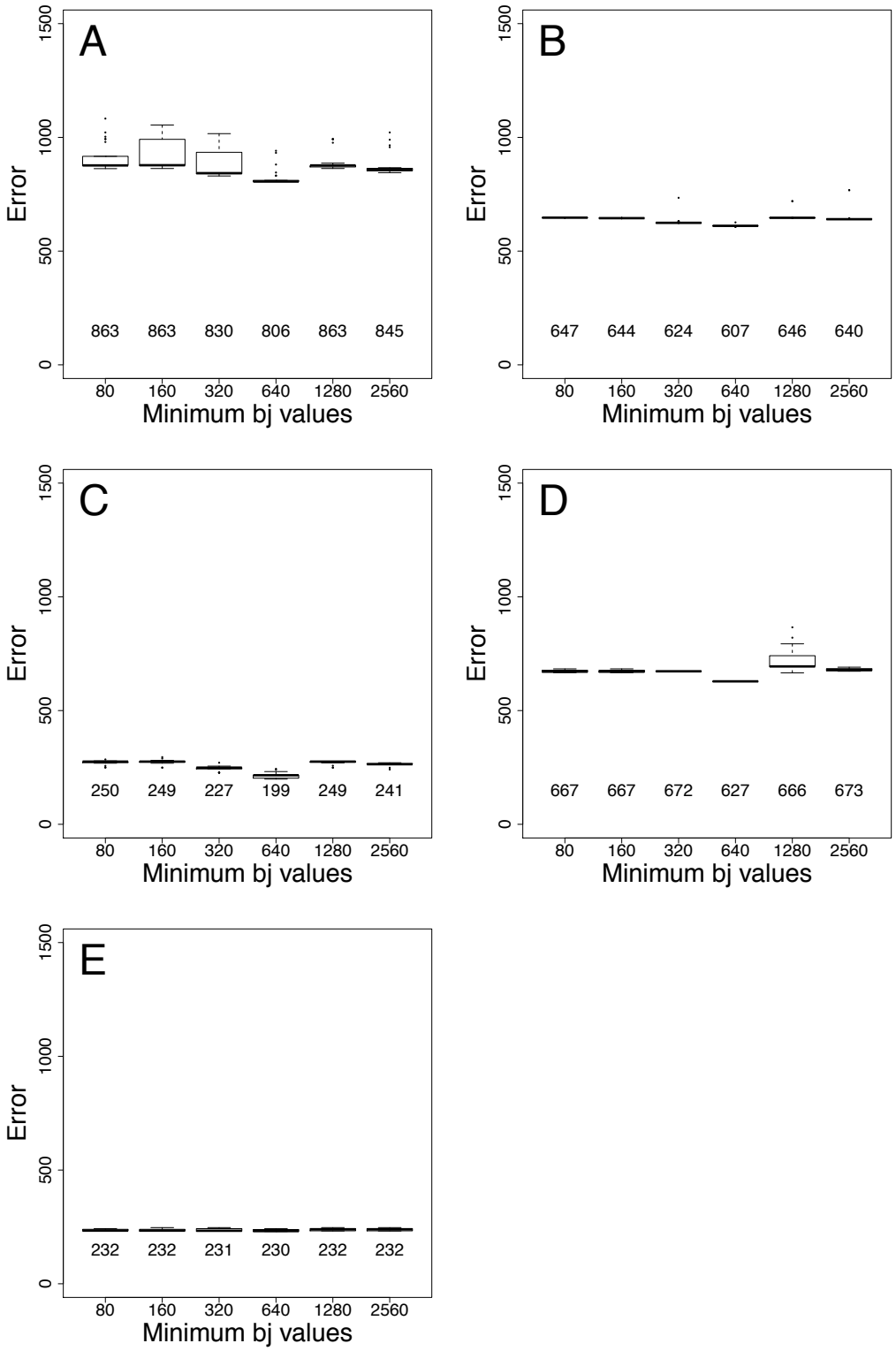

Fig. S11. Sensitivity testing of the minimum b_j values for the one-month NHP (**A**), three-month NHP (**B**), five-month NHP (**C**), human monovalent vaccine (**D**) and human natural infection (**E**) antisera maps. Plots show 200 runs of each map at each setting of b_j (ranging from 1:80-1:2560). The best minimum b_j is the one that allows for the best fit the data set, and thus has the lowest overall error.

Comparing the differences between the unadjusted and adjusted column basis maps, we found that overall, while there were some shifts of viruses on maps with the b_j values estimated in different ways, our main conclusions in the manuscript related to virus positions are still the same: the antigenic relationships among the DENVs are overall similar to maps without adjusting the b_j values, presented in the manuscript Figs. 2-4 (fig. S12 shows antigenic maps with each column adjustment for the three-month NHP data set). However, because the antisera shifted more with different b_j values, we tested all the main findings of our paper in relation to serum position using each of the column adjustment approaches described above (this is discussed in section 2.5).

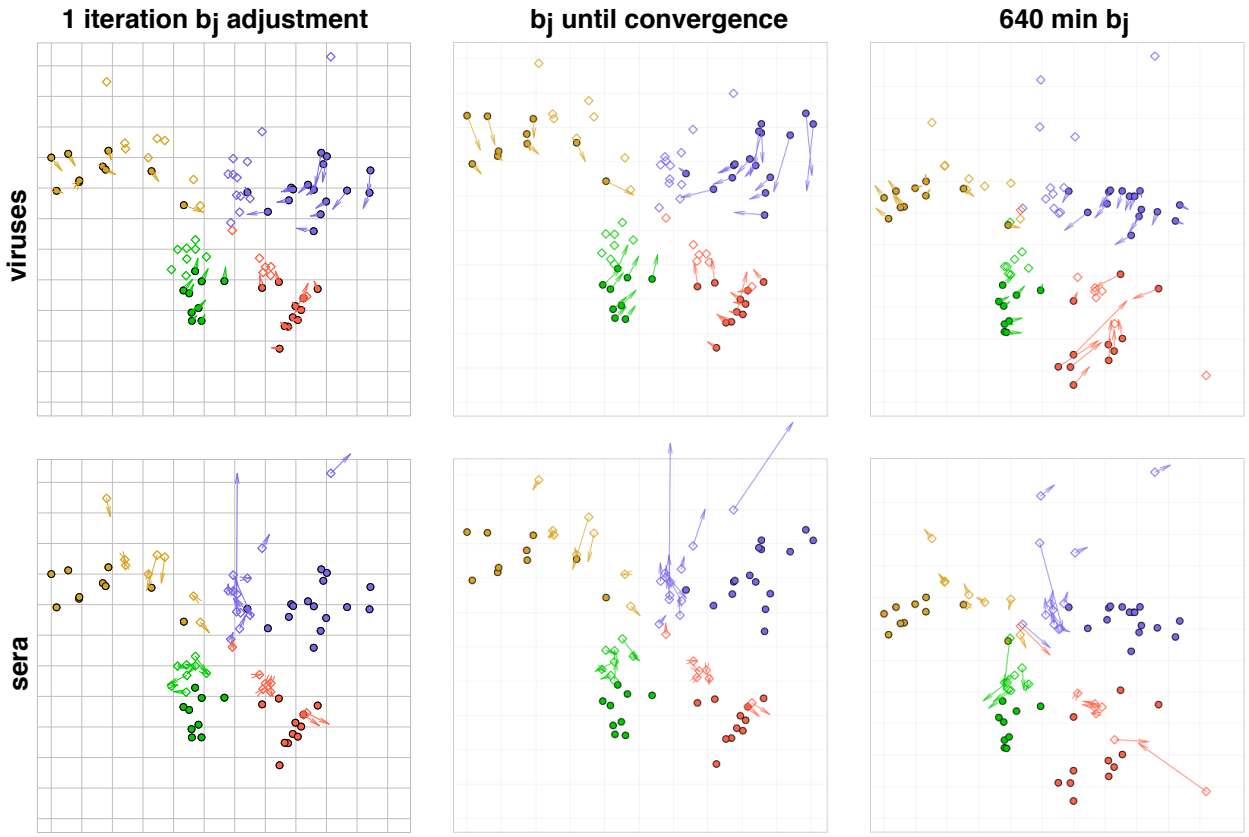

Fig. S12. Comparison of virus positions (**top**) and serum positions (**bottom**) for the three-month NHP map made with adjusted column bases (b_j values) to the unadjusted maps. The one iteration column adjust (**left**), converged column adjust (**center**), and minimum column basis set to 1:640 (**right**).

2. Antigenic analyses

2.1. Clustering of viruses and antisera in antigenic maps

2.1.1. DENV clustering analyses

Antigenic clusters on each antigenic map were estimated with the partitioning around medoids function (pamk) in R, a clustering method that is relatively robust to outliers. The optimal number of clusters was determined by pamk (estimated by the optimum average silhouette width) on map distances, and was found to be two clusters for the one, three, and five-month NHP maps as well as the human monovalent vaccine map. Four clusters optimally defined virus clustering on the human natural infection map, but these clusters did not directly correspond to current serotype categories. When we required pamk to identify four clusters on all maps, not all viruses were clustered together with other viruses of the same DENV type. This means that, although visually, when colored by serotype, the viruses may appear clustered, their relative positions on the map do not trivially fall into four clusters, as may have been expected from the serotype paradigm and genetic features of the strains.

For the one, three and five-month NHP maps, 41-55% of viruses were at least as close to a virus in another type as to some viruses of the same type (table S11). For the human monovalent vaccine map and the human natural infection map, 94% and 21%, of viruses, respectively, were at least as close to a heterologous type.

	Viruses to viruses				Sera to viruses			
Antigenic map	DENV1	DENV2	DENV3	DENV4	DENV1	DENV2	DENV3	DENV4
One-month NHP	1.1	4.3	0.9	2.7	17.4	3.3	5.6	4.3
Three-month NHP	3.4	2.8	1.6	2.3	4.1	6.9	1.7	7.9
Five-month NHP	0.9	2.1	1.7	2.1	3.4	4.2	1.2	1.5
Human monovalent vaccine	12.5	12	2.8	3.7	14.1	3.8	4.0	5.2
Human natural infection	1.1	1.6	0.7	2.1	1.7	2.9	33.6	3.4
One-year monkey (Russell and Nisalak (1967)	2.4	0.6	0.2	1.1	0.8	0.4	0.6	0.6
Late-convalescent traveler (Messer *et al.* 2012)	*	*	0.6	*	0.1	0.3	0.7	0.3
Human monovalent vaccine (Durbin *et al.* 2013)	*	*	*	*	*	*	*	*
Human monovalent vaccine (Vasilakis *et al.* 2008)	0.6	0.8	*	0.7	1.3	1.5	*	2.3
Peruvian epidemic (Kochel *et al.* 2002)	0.1	0.8	*	*	2.4	1.0	*	*

	Viruses to viruses					Sera to viruses				
Antigenic map	DENV1	DENV2	DENV3	DENV4	viruses	DENV1	DENV2	DENV3	DENV4	sera
One-month NHP	2	15	0	9	55%	6	6	5	6	64%
Three-month NHP	2	11	2	5	43%	3	11	5	6	69%
Five-month NHP	0	5	6	4	41%	1	6	1	2	63%
Human monovalent vaccine	7	13	8	6	94%	10	10	8	8	90%
Human natural infection	1	1	0	1	21%	3	1	3	4	55%

Table S11. Comparison of within and between type differences for all data sets. (**A**) The ratio of the maximum distance observed between points of the same type, to the minimum distance between any point of that type to any heterologous type. Values ≥1 indicate that the distance within type is greater than the distance between types. The ratio of within and between type difference from viruses to viruses (**left**) as well as the between antisera and viruses (**right**), for each DENV type. (**B**) The number of viruses or antisera of each type that are at least as close to one virus of a different type as to some viruses of the same type.

The maximum difference within a DENV type exceeded the minimum distance to a heterologous type for most clusters on the antigenic maps. The only exceptions were the DENV3 isolates on the one-month NHP and natural infection maps, as well as the DENV1 isolates on the five-month NHP map, which were more similar within type than between types (table S11, ratios ≥1 indicate greater spread within than between types). Overall, the antigenic clusters on all maps had ratios close to one, meaning that within and between-type spread is comparable.

2.1.2. Antiserum distances to homologous and heterologous DENV types

Because both viruses and antisera are positioned in antigenic maps, antigenic cartography can be used to study the breadth of the neutralizing responses of antisera. On all antigenic maps, the antisera are almost all more centrally located than viruses of the homologous type, meaning the sera are not clearly type-specific. For antisera raised against each DENV type, the maximum distance to a virus of the homologous type is greater than the distance to the closest heterologous virus (table S11). The ratio of within type to between type distance measured for each serum and averaged by cluster is near or greater than one for all DENV types on all maps (range of 0.9-9.4).

For the one-month antigenic map, the median antigenic distance between each antiserum and virus of the homologous type was significantly less than to heterologous viruses (table S12). However, the most poorly neutralized isolate of the homologous type was at least as far as the most similar heterologous virus. The median distances of the viruses used for infection from their respective antisera were significantly further than the closest homologous-type virus to antiserum, providing a basis for higher-than-homologous titers.

	Antigenic distances of antisera to viruses	Three-month range (median)	Wilcoxon rank signed test
A	Median homologous	1.2-5.9 (2.0)	
	Median heterologous	3.2 - 9.7 (4.5)	$p<0.001$
B	Maximum homologous	1.8-7.1 (3.5)	
	Minimum heterologous	0.6-7.9 (1.8)	$p<0.001$
C	Infecting virus	0.4-5.3 (2.3)	
	Minimum homologous	0.2-5.1 (1.0)	$p<0.001$

Table S12. Summary statistics on the breadth of neutralizing responses by antisera to viruses of homologous and heterologous types for the one-month antigenic map. For each antiserum, we estimated: (**A**) the median distance to viruses of homologous and heterologous types, (**B**) the maximum distance to a homologous and minimum distance to a heterologous type, and (**C**) the distance to the infecting isolate and minimum distance to a virus of the homologous type. The range of these values and median value for all antisera are shown. A Wilcoxon rank signed test compared these metrics across the antisera.

2.2. Analyses of one, three, and five-month NHP antisera data sets

2.2.1. Changes in DENV antigenic relationships over time

The neutralizing response following primary DENV exposure is described as narrowing to the homologous DENV type in the months after infection: if so, then antisera drawn soon after infection may identify the DENV types as diffuse antigenic clusters, while antisera drawn later may recognize the DENVs as discrete serotypes. We tested if serially sampled NHPs changed in how they recognized the antigenic relationships among the DENV panel over time. We used antisera from 36 NHPs one and three months after experimental inoculation, and from a subsample of NHPs (n=16) five months after inoculation. All antisera drawn at one month were titrated against the full DENV panel (n=47), including all isolates used for infection (n=35). The three-month antisera were titrated against nearly the full DENV panel (n=46). The five-month antisera were titrated against all antigenically diverse representatives of the DENV panel and all homologous isolates for the 16 NHPs for which antisera was available at five months (n=37). We compared the antigenic relationships among DENVs as recognized by one and three-month antisera (46 viruses in common) and three and five-month antisera (37 viruses in common) by extracting the pairwise differences between all viruses on each map, and plotting the distances for all corresponding virus pairs for each month (fig. S13). Distances between isolates on identical maps would be linearly related, with slope of one, and intercept of zero.

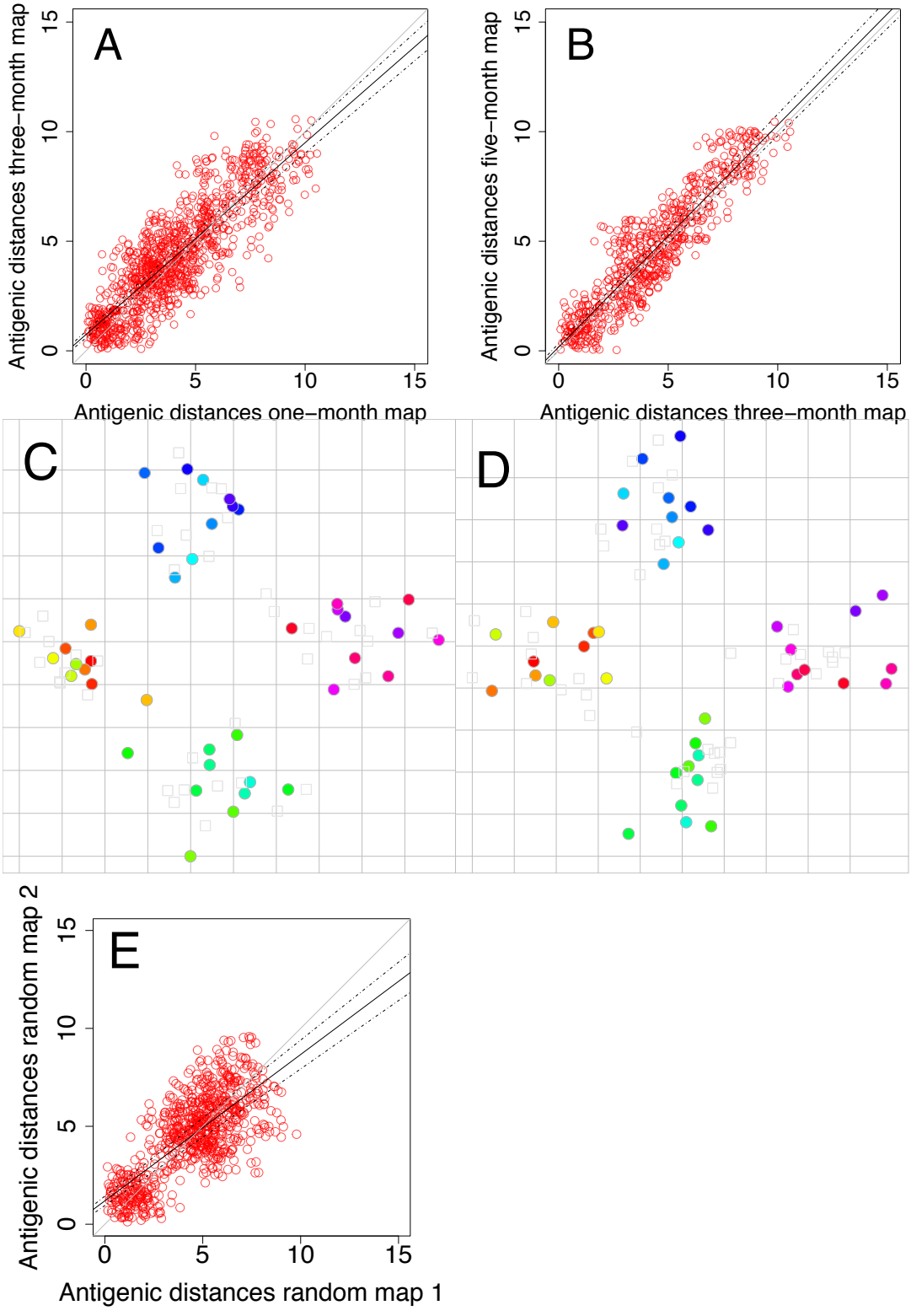

Fig S13. Plots of the pairwise distances between all viruses in the one-month NHP map compared to same distances between corresponding viruses in the three-month NHP map (**A**), and the pairwise

distances between all viruses in the three-month compared with those in the five-month NHP maps (**B**). Two example 'random' simulated antigenic maps, made by randomly positioning viruses within each cluster, are also shown (**C-D**), and the pairwise differences between corresponding isolates on those two random maps is shown (**E**). The black lines in figures A, B, and E represent the linear regression of the pairwise distances between maps, and dotted lines the 95% confidence interval of the linear regression. The grey line represents perfect correspondence between maps.

The distance between any two viruses at one-month differed from the distance between the same isolates on the three-month map by an average of 1.30 AU, equivalent a 2.5-fold difference in the neutralization assay (table S13). The three and five-month maps were even more similar: pairwise differences between any two viruses at three months were, on average, only 1.06 AU (2.1-fold) from the distance between isolates at five-months.

As a comparison, we produced simulated antigenic maps with isolates randomly positioned within each cluster and conducted the same pairwise virus position analysis (fig. S13). The simulated maps were designed to have similar clustering patterns to the DENV maps we observed, but on these maps, isolates of each DENV type were randomly positioned within the cluster. The average correspondence between pairwise isolates on any two random maps was 1.61 AU, worse than the correspondence seen between the NHP maps (table S13).

	Average disagreement between map distances
Pairwise distances between viruses at:	
One vs. three months	1.30
Three vs. five months	1.06
Viruses on any two random maps	1.61
Pairwise distances between antisera at:	
One vs. three months	2.14
Three vs. five months	0.86

Table S13. The Average difference in antigenic distance between pairwise viruses (**top**) or antisera (**bottom**) on the one-month compared to three-month NHP maps, or the three-month compared to five-month NHP maps. We also compared the antigenic distance correspondence between 10 simulated maps with viruses randomly position within each cluster.

We thus found that there are only modest changes in the antigenic relationships of DENVs recognized by one and three-month panels of NHP antisera, and few changes between the three and five-month antisera. Even with the changes observed, the DENV types grouped as diffuse antigenic clusters on antigenic maps at all three time points.

Between one and three months after infection, B cells are still in the process of affinity maturation and selection. The three-month map is thus more likely to be representative of the long-lived antibody population. It is interesting that the three and five-month maps are much more similar to one another than the one to three-month maps, suggesting that the properties of

antibodies constituting the antisera change minimally between three and five months. We thus conclude that early and late convalescent antisera recognize similar underlying antigenic properties in the DENV panel, although some shifts are observed between one and three months.

2.2.2. Changes in NHP neutralizing responses over time

The short-term, immediate immune response to DENV infection is described as broadly neutralizing, but is thought to narrow in specificity to the infecting type in the ensuing months, thus only providing long-term protection against the infecting DENV type. This is consistent with epidemiological observations: limited protection is observed against heterotypic DENV types for up to two years, after which individuals are at increased risk of severe disease (*29*, *49*–*52*). However, although the trajectories of neutralizing responses are described in the literature as becoming increasingly type-specific, the degree to which changes are due to a general decrease of antibody titers or, alternatively, a result of increasing type-specificity of neutralizing antibodies in an antiserum sample, is not well understood. We attempted to distinguish between changes in magnitude and changes in specificity for the NHPs at one, three, and five months after infection.

We first measured the average change in magnitude of neutralizing titers for each NHP between one and three months, and three and five months (table S14). The majority of NHPs had either stable or declining neutralizing titers between one, three, and five months. Notably, five NHPs had significantly higher neutralizing titers at three than one month, perhaps due to the development of more potently neutralizing antibodies through affinity maturation.

NHP	1:3 months	p-value	3:5 months	p-value
DEN1_Nauru_1974_NIHvaccine	0.96	0.69	0.94	0.48
DEN1_VietNam_2008_BID_V1937	1.09	0.52	1.06	0.64
DEN1_Thailand_1964_16007	*	*	*	*
DEN1_PuertoRico_2006_BID_V852	1.55	<0.01	0.64	<0.01
DEN2_Tonga_1974_NIHvaccine	0.82	0.08	0.76	0.02
DEN2_VietNam_2006_31_178	0.57	0.01	0.71	<0.01
DEN2_Vietnam_2003_AC21	0.65	<0.01	0.85	0.04
DEN2_Nicaragua_2005_BID_V533	0.68	<0.01	0.97	0.65
DEN2_Nicaragua_2006_BID_V571	1.33	0.02	0.72	0.01
DEN2_Peru_1996_IQT2913	0.69	0.01	0.81	0.02
DEN2_Vietnam_2006_BID_V735	2.35	<0.01	0.87	0.40
DEN2_Malaysia_2008_DKD811	0.82	0.12	0.79	0.01
DEN3_Fiji_1992__	0.64	<0.01	1.02	0.77
DEN3_Vietnam_2006_BID_V1329	1.09	0.44	0.76	<0.01
DEN3_Vietnam_2007_BID_V1817	1.01	0.91	0.96	0.66
DEN4_PuertoRico_1999_BID_V2446	0.86	0.20	0.98	0.85
DEN4_Indonesia_1973_M30153_p5	0.77	0.01	0.91	0.32
DEN1_Peru_2000_IQT_6152	2.37	<0.01	*	*
DEN1_Cambodia_2003_GenBankGQ868619	1.14	0.13	*	*
DEN1_Bolivia_2010_FSB_3363	1.15	0.17	*	*
DEN1_Venezuela_2000_OBT_1298	0.93	0.11	*	*
DEN1_Burma_2005_61117	0.97	0.77	*	*
DEN2_Vietnam_2003_AC21_2	0.95	0.18	*	*
DEN2_Cambodia_2009_D2T0601085_KH09_KSP	0.91	0.44	*	*
DEN2_Senegal_2003_Sendak_HD_0674	0.81	0.02	*	*
DEN2_Vietnam_2006_32_135_2	0.88	0.26	*	*
DEN3_Nicaragua_2009_608	0.92	0.26	*	*
DEN3_PuertoRico_1963_PRS_228762	0.95	0.41	*	*
DEN3_Cambodia_2011_V0907330	1.22	0.03	*	*
DEN3_PuertoRico_2006_429965	1.06	0.43	*	*
DEN3_Burma_2008_80931	1.10	0.20	*	*
DEN4_Cambodia_2010_U0811386	1.10	0.34	*	*
DEN4_Malaysia_1973_P73_1120_sylvatic	0.88	0.07	*	*
DEN4_Cambodia_2011_V0624301	0.98	0.82	*	*
DEN4_Burma_2008_81087	0.90	0.05	*	*
DEN4_Nicaragua_1999_703	1.24	0.06	*	*
DEN4_Brazil_2012_BR_12	1.14	0.21	*	*

Table S14. Changes in the magnitude of neutralizing antibodies for each NHP over time against the DENV panel. For each antiserum, a paired t-test was done to compare all titers against viruses at one month to three months, as well as titers from three months to five months (mean difference and p-values are shown).

To identify changes in the type-specificity of each NHP, we compared antiserum positions for each NHP in the one, three, and five-month maps. The antiserum positions for most NHP changed dramatically between one and three months (Fig. 4A). The correspondence in relative positioning in the antigenic maps between antisera at one and three months was poor, with each serum differing by an average of 2.14 AU between maps (fig. S14 and table S13).

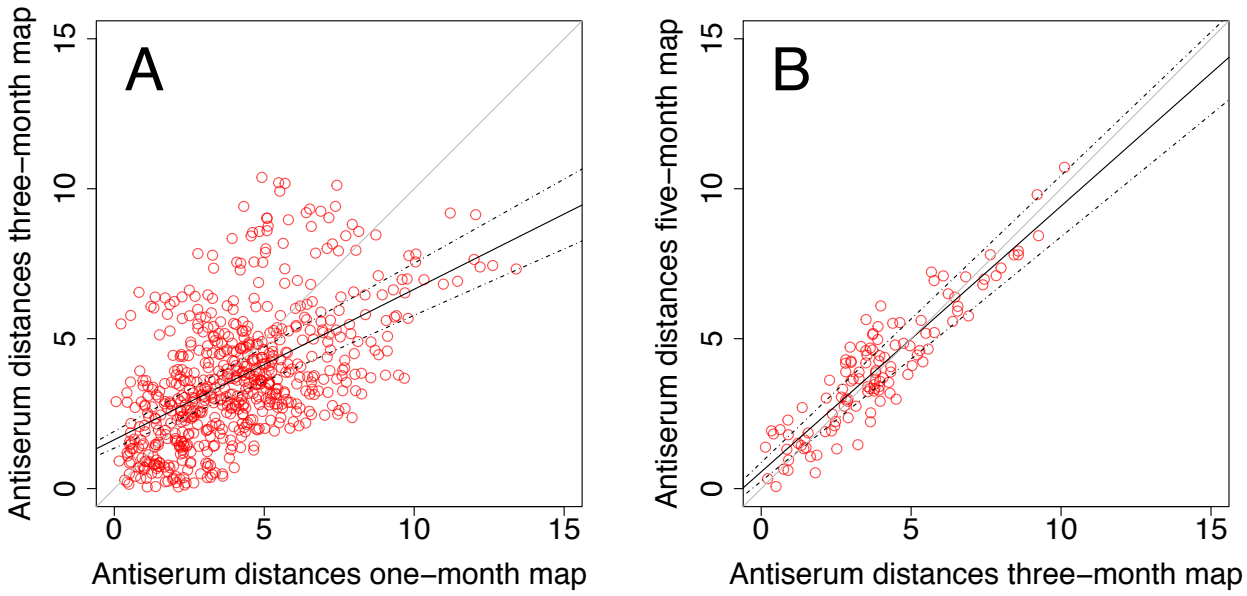

Fig S14. Plots of the pairwise distances between all antisera in the one-month compared to same distances between corresponding antisera in the three-month NHP map (**A**), and the pairwise distances between all antisera in the three-month compared with the five-month NHP maps (**B**). The black lines represent the linear regression of the pairwise distances between maps, and dotted lines, the 95% confidence interval of the linear regression. The grey line represents perfect correspondence between maps.

We did not, however, find evidence for a systematic shift toward increasing type-specificity. Only a few antisera moved away from heterotypic clusters and toward the center of the homologous type, which would be expected for increased type-specificity. The majority of antisera shifted in specificity in relation to the DENV panel, but not in any one direction. The average direction of change for each cluster (black arrows) is shown in Fig. 4A: DENV1 and DENV3 infection antisera shifted closer to the center of each cluster, while DENV2 and DENV4 moved toward the center of the map. Further, of the five NHPs whose neutralizing titers increased between one and three months, only 3/5 of the antisera increased in type-specificity, suggesting that even for antisera with improved neutralizing potency, antisera do not necessarily become more type-specific.

Between three and five months, the neutralizing responses either stayed the same or dropped in magnitude, with half of the NHPs exhibiting stable titers while the other half had a substantial drop in titer levels (table S14). However, the antiserum positions changed very little between three and five months, each moving, on average, by only 0.86 AU on the map. Of those small shifts, there was not a detectable trend toward increasing specificity, with very short arrows for the average movement of antisera per cluster (Fig. 4B).

Finally, we directly plotted the trajectories of neutralizing titers at one, three and five months for each NHP against the DENV panel as a visual check that indeed the neutralizing responses were not systematically becoming more type-specific over time (fig. S15).

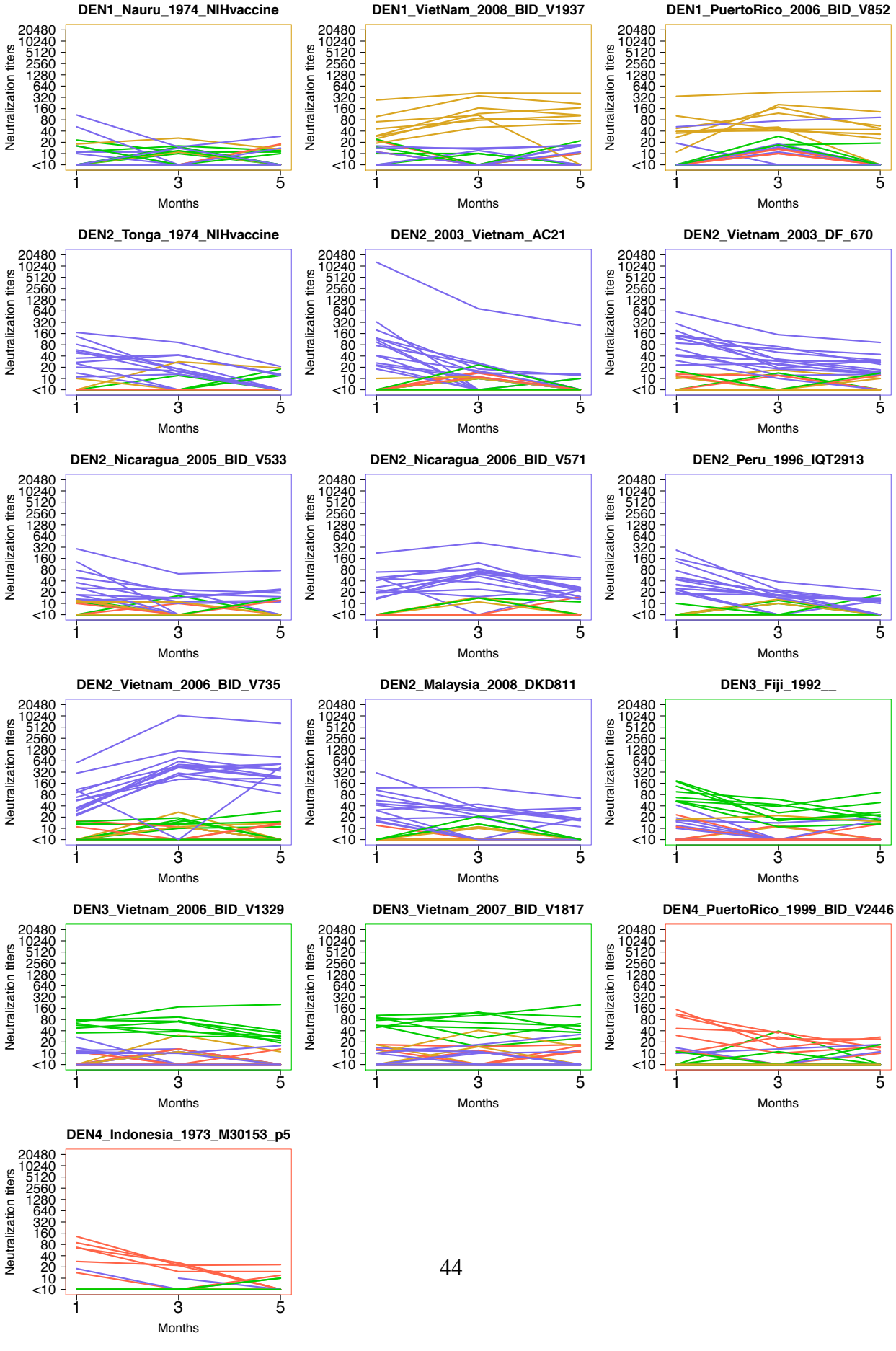
DEN1_Nauru_1974_NIHvaccine
DEN1_VietNam_2008_BID_V1937
DEN1_PuertoRico_2006_BID_V852
DEN2_Tonga_1974_NIHvaccine
DEN2_2003_Vietnam_AC21
DEN2_Vietnam_2003_DF_670
DEN2_Nicaragua_2005_BID_V533
DEN2_Nicaragua_2006_BID_V571
DEN2_Peru_1996_IQT2913
DEN2_Vietnam_2006_BID_V735
DEN2_Malaysia_2008_DKD811
DEN3_Fiji_1992__
DEN3_Vietnam_2006_BID_V1329
DEN3_Vietnam_2007_BID_V1817
DEN4_PuertoRico_1999_BID_V2446
DEN4_Indonesia_1973_M30153_p5
Neutralization titers
20480
10240
5120
2560
1280
640
320
160
80
40
20
10
<10
1
3
5
Months

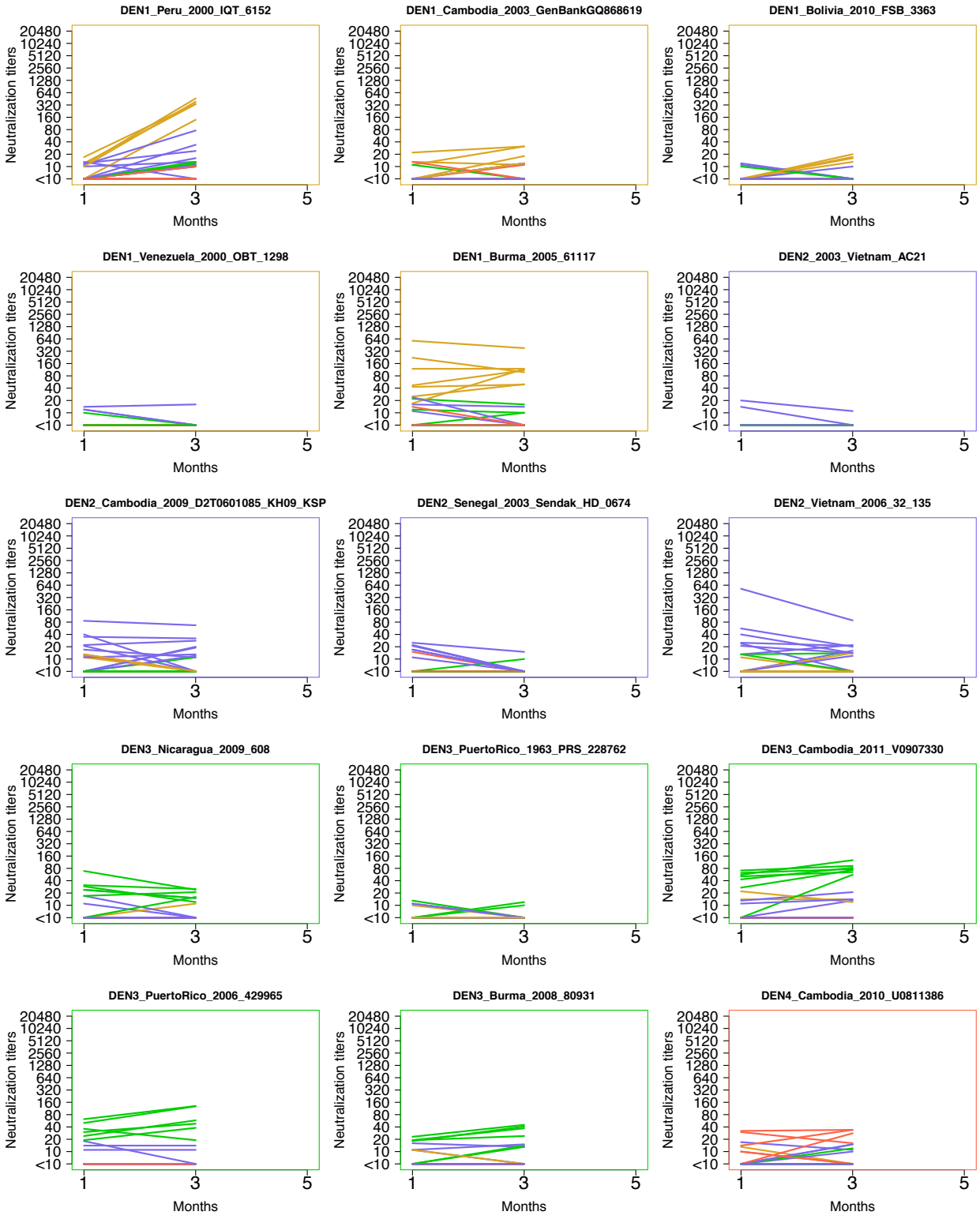
DEN1_Peru_2000_IQT_6152
DEN1_Cambodia_2003_GenBankGQ868619
DEN1_Bolivia_2010_FSB_3363
DEN1_Venezuela_2000_OBT_1298
DEN1_Burma_2005_61117
DEN2_2003_Vietnam_AC21
DEN2_Cambodia_2009_D2T0601085_KH09_KSP
DEN2_Senegal_2003_Sendak_HD_0674
DEN2_Vietnam_2006_32_135
DEN3_Nicaragua_2009_608
DEN3_PuertoRico_1963_PRS_228762
DEN3_Cambodia_2011_V0907330
DEN3_PuertoRico_2006_429965
DEN3_Burma_2008_80931
DEN4_Cambodia_2010_U0811386
Neutralization titers
20480
10240
5120
2560
1280
640
320
160
80
40
20
10
<10
1
3
5
Months

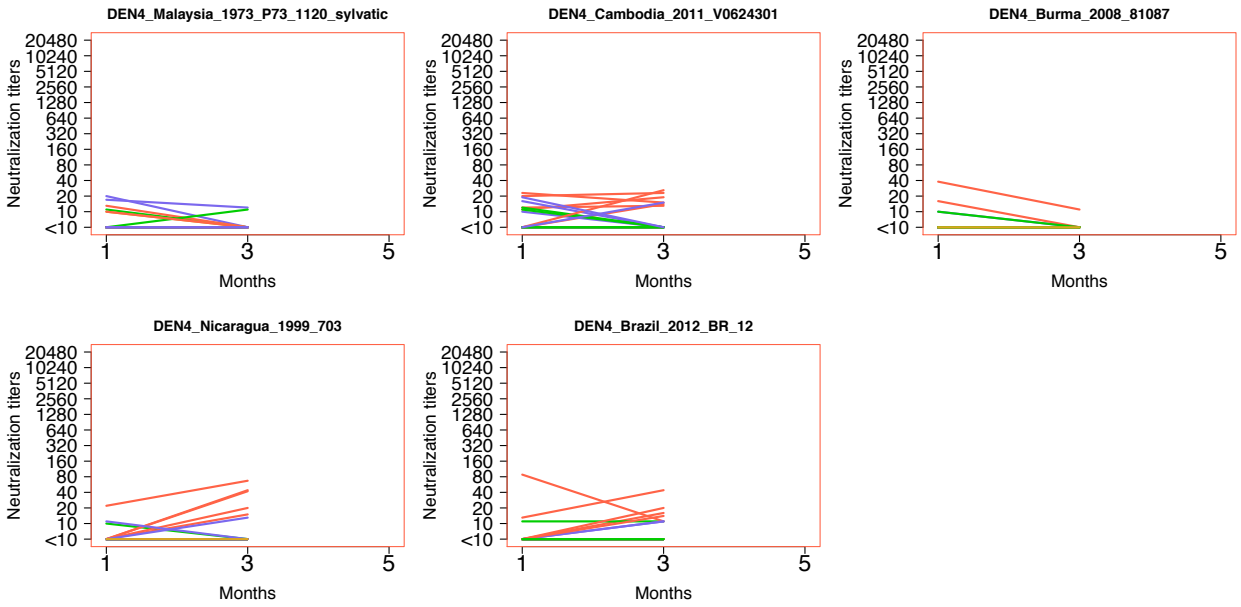

Fig. S15. Plots of the trajectories of neutralization titers for each NHP against the DENV panel at one, three, and five months after infection. Each virus trajectory line is colored by the DENV type: DENV1=yellow, DENV2=blue, DENV3=green, DENV4=red.

We thus found that although neutralization titers drop in absolute magnitude, in some cases below the limit of assay detection, there was not evidence for a systematic shift toward increasing specificity to viruses of the infecting type and decreasing specificity toward heterotypic viruses. Most individuals maintain specificity between three and five months, but these responses were not all type-specific. For researchers looking at neutralization data with a higher titer threshold for detection (>1:40, for example) and using single representatives of each DENV type, the observation of a drop in magnitude of neutralization titers may not be distinguishable from increasing type-specificity.

2.3. Human natural infection antigenic maps with titrations conducted on mosquito compared with human cells, at one and two years post-infection

The titrations used to make the human natural infection map in Fig. 3B were conducted using the immunofocus reduction neutralization test on C6/36 (mosquito) cells. However, all the human natural infection antisera were also measured for neutralizing antibodies using a flow-cytometry based-assay on Raji DC-SIGN cells (a human cell line with expression of DC-SIGN, an important receptor for DENV attachment) using reporter virus particles (RVPs) representing each of the four DENV types (*50*).

We tested if we observed more cross-reactive neutralization titers using the C6/36 cell assay (Fig. 3B) than with the Raji DC-SIGN cell assay. We compared the antigenic map of the 14-virus DENV panel titrated on C6/36 cells to the antigenic map of the RVP viruses titrated against each child's antisera in the Raji DC-SIGN cell assay (fig. S16). Overall, most antisera were in approximately the same position on the Raji map as the C6/36 map, with only a handful of antisera shifting by more than two antigenic units. Notably, the DENV4 cluster, which is in a different position than in the antigenic maps of the one, three, and five-month NHP antisera as well as the monovalent vaccine antisera, is in the same position on both the Raji and C6/36 human natural infection antisera maps. This suggests that the Nicaraguan antisera recognized the antigenic relationships among the DENVs slightly differently from the other antisera panels. This may be because the children in Nicaragua were infected with similar isolates, and the isolates circulating in Nicaragua induce neutralizing responses that recognize more similarity between DENV1 and DENV4.

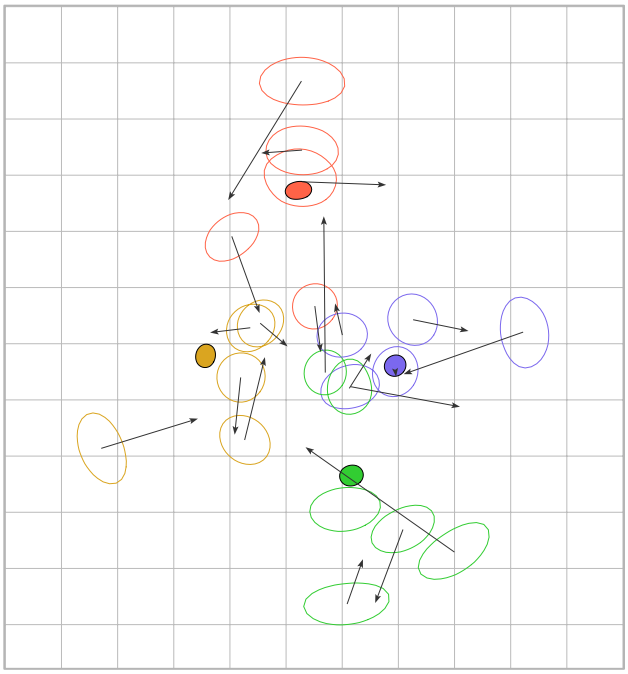

Fig. S16. An antigenic map of the 20 human natural infection antisera titrated against RVP representatives of each DENV type on Raji DC-SIGN cells in a flow-cytometry system. Arrows point to

the positions of the antisera on the antigenic map of the 14-virus DENV panel titrated on C6/36 cells in Fig. 3B.

Where data were available, we also checked the neutralization titers estimated with the RVP assay two years after primary infection (fig. S17). We find no evidence that individuals became more type-specific over this period, and overall, most maintained their individual pattern of reactivity observed in the first year after infection. We made antigenic map of the RVP titrations for antisera drawn two years after infection and compared them to the RVP map of antisera from one year after infection; overall, the shifts are relatively small, and do not indicate that the individuals are becoming increasingly type-specific over time (fig. S18).

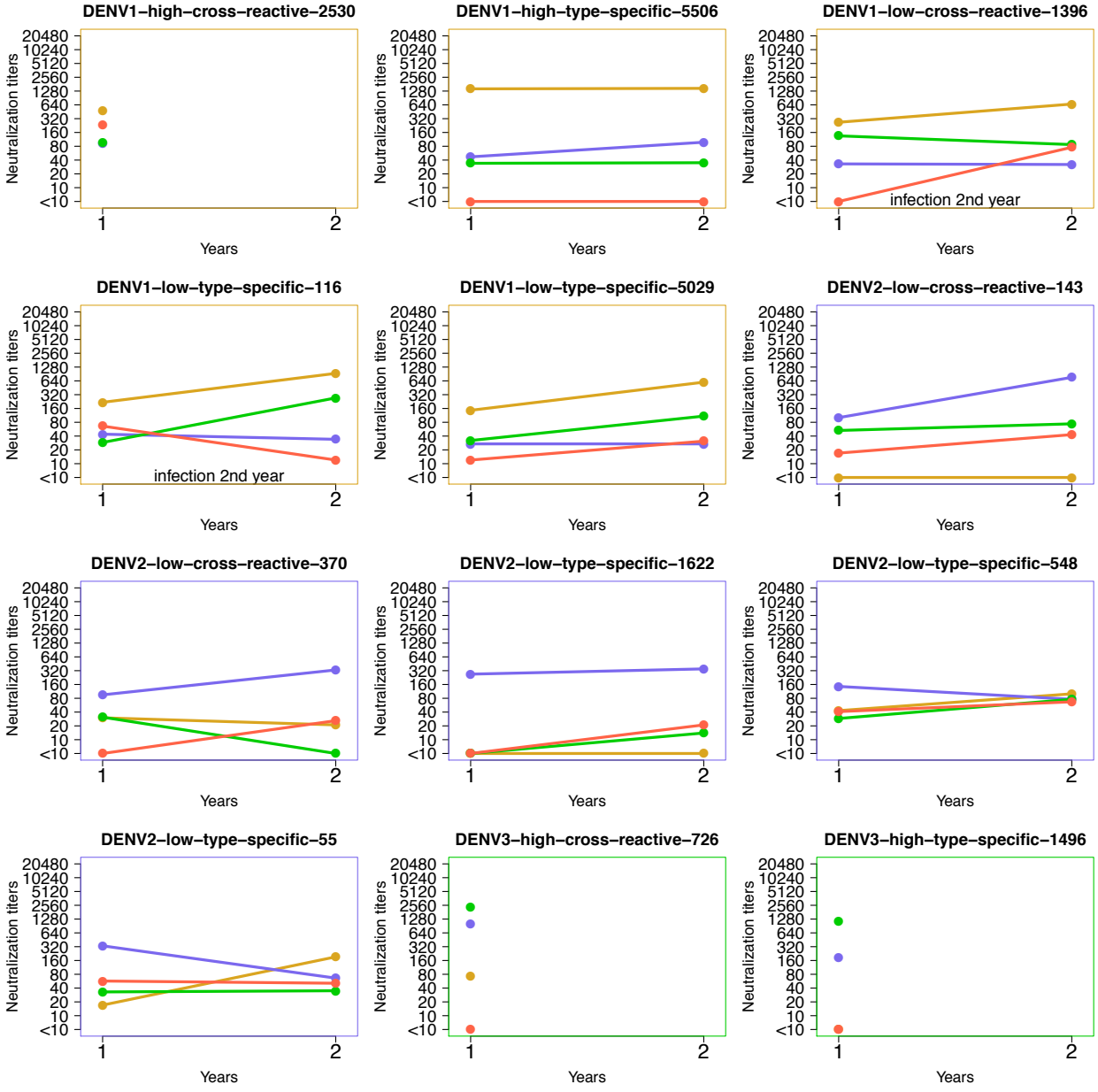

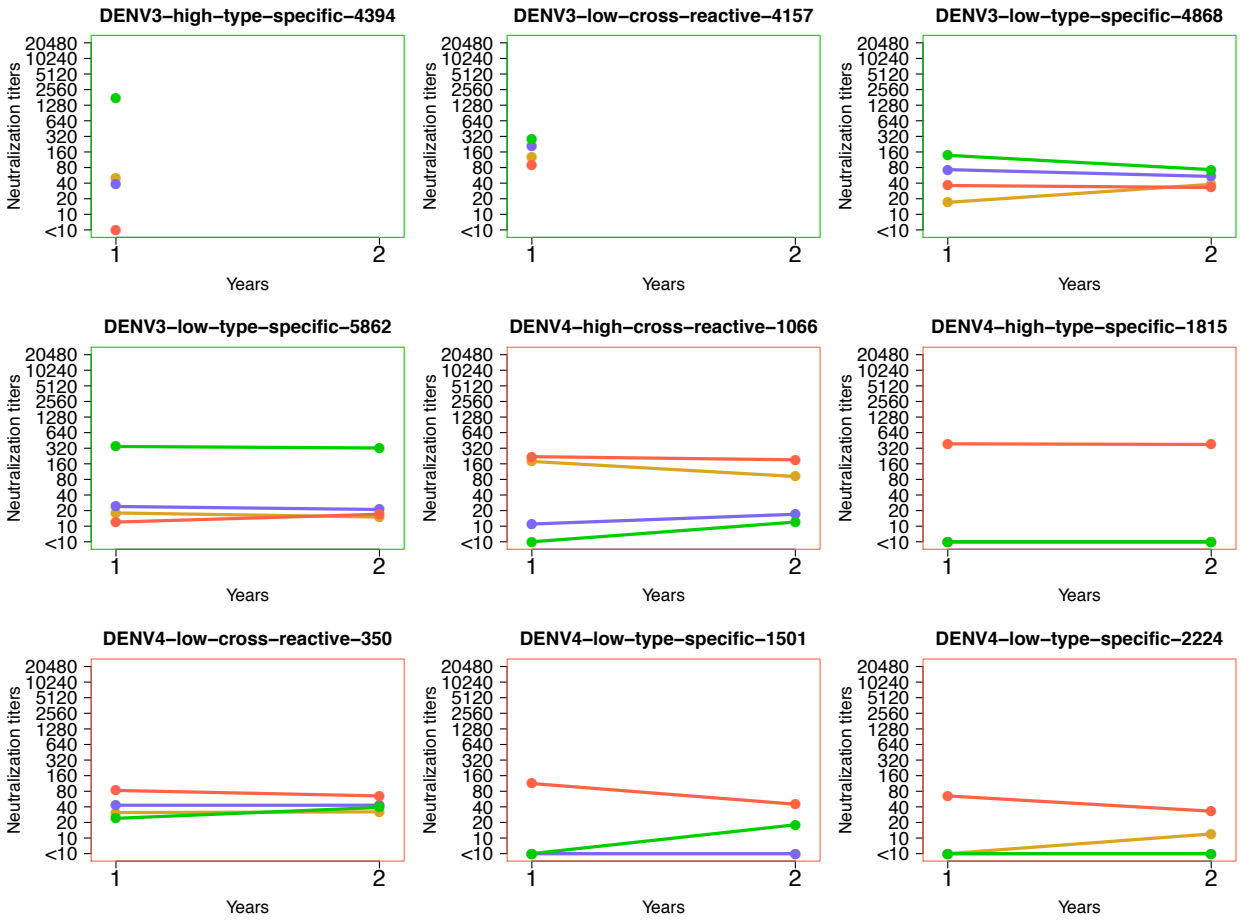

Fig. S17. Plots of the neutralizing antibody trajectories of each naturally infected child against the four RVPs (DENV type: DENV1=yellow, DENV2=blue, DENV3=green, DENV4=red) at one and two years after primary infection. Two individuals (labeled) had second infections in year two.

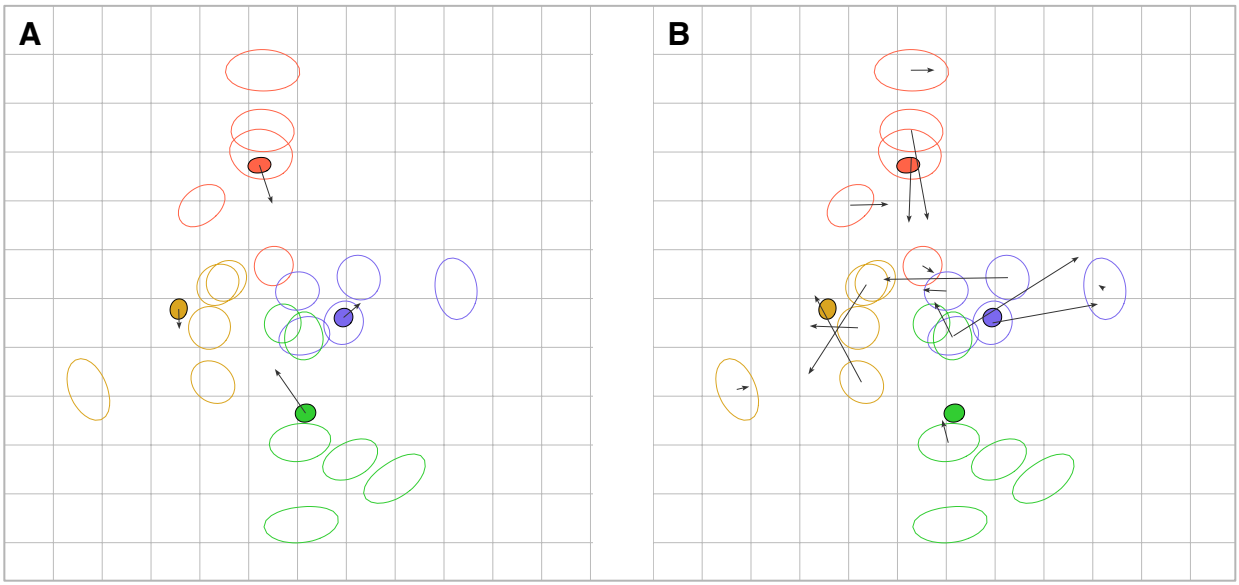

Fig. S18. The antigenic map made with the RVP titrations for natural infection antisera drawn one year after infection compared to the position of the RVPs (**A**) and antisera (**B**) two years after infection.

2.4. Analyses of antiserum positions in the human monovalent vaccine antigenic map

The antisera samples from human volunteers who received the monovalent components of the NIH live attenuated dengue vaccine provided the unique opportunity to test how multiple individuals inoculated with the same antigen recognized the antigenic relationships among the DENV panel. As with the NHP and human natural infection antigenic maps, the antisera from each of the four monovalent vaccine trial groups were scattered among the isolates on the antigenic map, and ranged in response from type-specific (peripheral on the map) to cross-reactive (central on the map) (Fig. 3A).

We conducted two experiments to test if distinct subsets of the antisera identified similar antigenic relationships among the DENV panel. First, we made antigenic maps using random subsets of the data containing three-quarters of the full antisera panel. We did this test ten times, and on each of the ten independent maps, the antigenic relationships among the DENV panel were very similar, with only a few viruses moving relative to their positions on the map with the full set of antisera (fig. S19).

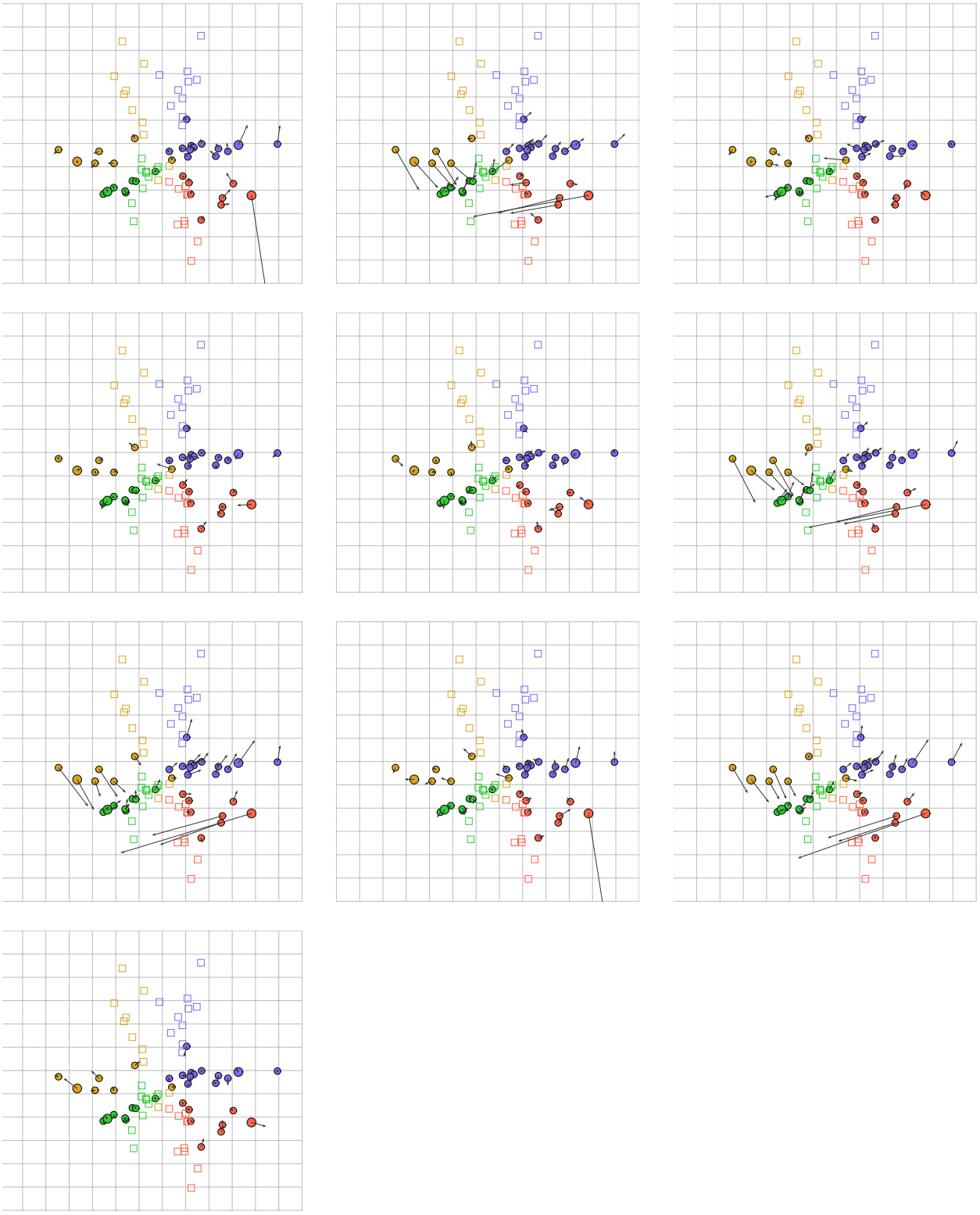

Fig. S19. The full human monovalent vaccine antigenic map from Fig. 3A, with arrows pointing to the position of isolates on maps made random subsets of the data containing three-quarters of the full antisera panel.

For our second experiment, we divided the antisera into two groups: the most type-specific half (the five most peripheral antisera for each DENV type) and the most cross-reactive half (the most central for each DENV type), based on the antigenic map made with all antisera. The relationships among the DENV panel differed little between the maps made with only the most central, cross-reactive 20 antisera or only the most peripheral, type-specific 20 antisera (fig. S20). This suggested that both the cross-reactive and type-specific neutralizing responses recognize similar antigenic relationships among the viruses.

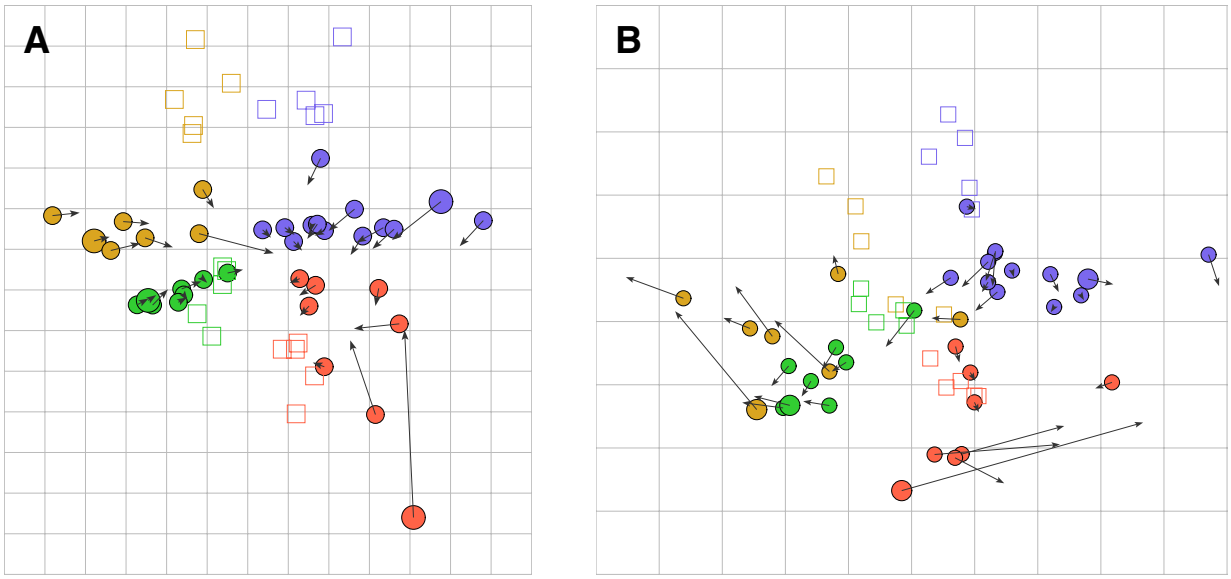

Fig. S20. The human monovalent vaccine antigenic map made with only the 20 most peripheral, type-specific antisera (**A**) or only the most central, cross-reactive antisera (**B**). Arrow point to the position of isolates map of the full data set, in Fig. 3A.

2.5. Interpretation of antigenic maps with adjusted column bases, b_j

For the analyses presented above in Section 2, the column basis b_j was set to the maximum titer for each antiserum, here called column unadjusted maps. Because the value of the column basis b_j can affect the interpretation of antigenic maps, we tested if we would reach the same conclusions in each of our analyses if we had used a different criterion for defining the column basis for each antiserum. Thus for the analyses above, we compared our results to those that would be observed if we optimized the b_j for each antiserum serum (one iteration or fully converged, explained above in Section 1.5.7), or used an absolute minimum for the value of b_j (set to a neutralization titer of 1:640, based on analyses described in Section 1.5.7).

First, we considered how our interpretation of the distance within and between DENV clusters would be affected. When b_j values were adjusted (one iteration or converged) for each antiserum, the antisera shifted toward the center of the map and the viruses moved further out toward the periphery (fig. S11). Thus the DENV isolates formed slightly more distinct clusters, although some viruses on all maps were at least as close to a heterologous isolate as some homologous isolates (table S15).

For the map with the minimum column basis set to 1:640, a slightly smaller proportion of the isolates, compared to the column unadjusted maps, were at least as close to a heterologous isolate as some homologous isolates (table S15).

Conversely, the antisera were actually more likely to be positioned as close to a heterologous isolate as some homologous isolates with the adjustment of b_j for each antiserum, as well as when setting the minimum column basis to 1:640.

A.	% of viruses	% of antisera
No bj adjustment		
One-month NHP	55%	64%
Three-month NHP	43%	69%
Five-month NHP	41%	63%
Human monovalent vaccine	94%	90%
Human natural infection	21%	55%
One iteration bj adjustment		
One-month NHP	38%	69%
Three-month NHP	26%	75%
Five-month NHP	19%	69%
Human monovalent vaccine	89%	95%
Human natural infection	7%	60%
bj until convergence		
One-month NHP	32%	75%
Three-month NHP	20%	72%
Five-month NHP	14%	69%
Human monovalent vaccine	75%	95%
Human natural infection	7%	65%
640 min bj		
One-month NHP	51%	69%
Three-month NHP	39%	78%
Five-month NHP	22%	75%
Human monovalent vaccine	92%	90%
Human natural infection	64%	75%

	Pairwise distances between viruses at:		**Pairwise distances between antisera at:**	
B.	One vs. three months	Three vs. five months	One vs. three months	Three vs. five months
No bj adjustment	1.30	1.06	2.14	0.86
One iteration bj adjustment	1.17	1.04	2.09	0.74
bj until convergence	1.26	1.10	1.40	0.71
640 min bj	1.36	1.97	2.09	1.43

Table S15. Comparison of results with column unadjusted antigenic maps and those made with adjusted column bases (b_j values), including a one iteration column adjust, converged column adjust, and minimum column basis set to 1:640.

We also tested if the relationships between viruses at one and three months and three and five months would be affected by different column basis values (table S15). The single iteration column adjusted maps, when compared to one another, actually had the greatest correspondence in distance between pairwise viruses. For serum position, the fully converged column adjusts had the best correspondence in pairwise antiserum distances. Overall, the correspondence estimates were similar or better for maps with adjusted column bases.

We also investigated whether antisera still showed evidence of becoming increasingly type-specific with the adjusted column bases (fig. S21). The arrows either point in the same direction as observed on the column unadjusted map, or actually move further toward the center of the map and away from the cluster, as in the case of the minimum column basis set to 1:640 maps at three and five months. Thus our conclusions are the same even with a column adjustment.

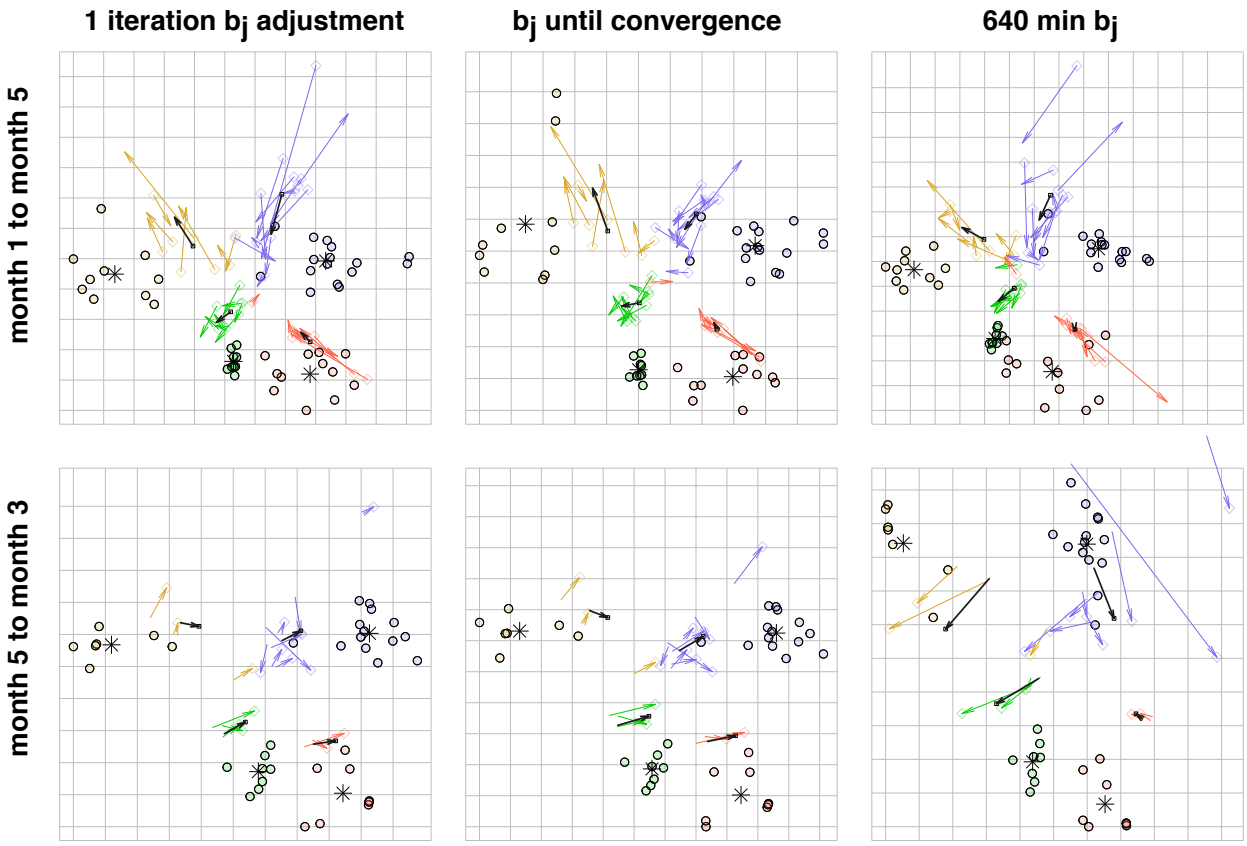

Fig. S21. One-month NHP map (**top**) and five-month NHP map (**bottom**) with adjusted column bases (b_j values): one iteration column adjust (**left**), converged column adjust (**center**), and minimum column basis set to 1:640 (**right**). Arrows are colored by DENV type (DENV1=yellow, DENV2=blue, DENV3=green, DENV4=red), and show changes in serum position over time, from one to three months (**top**) and from three to five months (**bottom**). The black arrows show the average shift in serum position for each cluster. The star denotes the center of the DENV antigenic cluster.

Finally, we considered if the antisera defined as most type-specific and most cross-reactive on the monovalent vaccine map without a column adjust would still be as distinct on the map with column adjustment. We took the extreme case, the fully converged column adjusted map, and drew arrows to the positions of the most type-specific antisera on the non-adjusted map, and the more cross-reactive on the non-adjusted map (fig. S22). Some of the antisera that were most type-specific before the column adjust had moved inward so that the antisera were

more clustered on the column adjusted map. Thus with the column adjust, there was slightly less distinction between the type-specific and cross-reactive antisera.

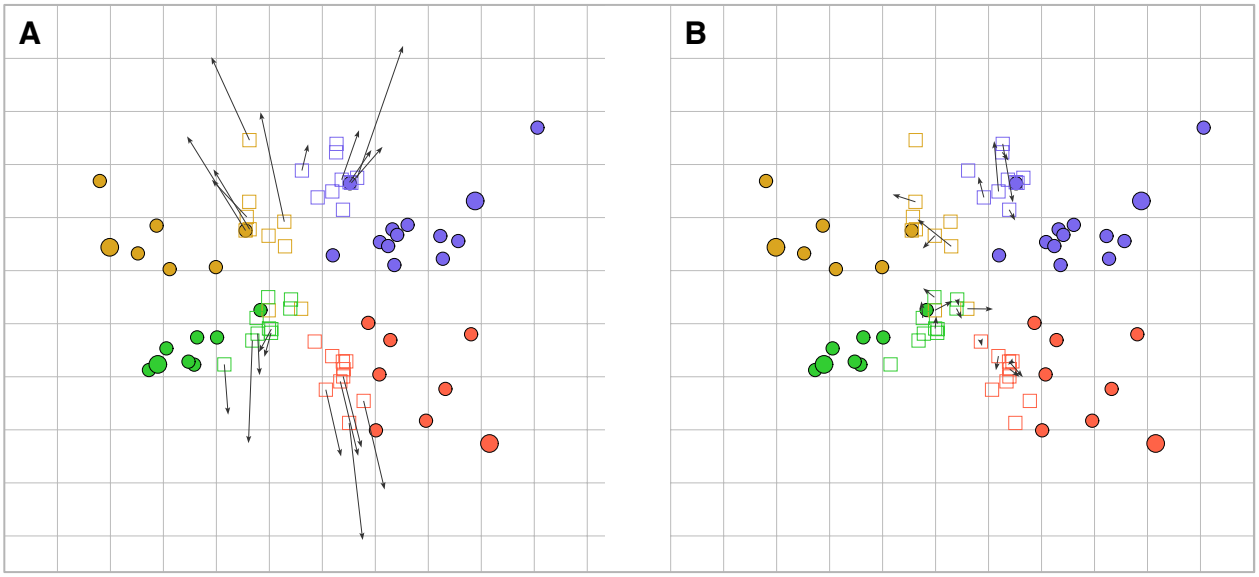

Fig. S22. The human monovalent vaccine antigenic map with converged column adjusted b_j values. Arrows point to the positions of the antisera that were most peripheral (**A**) and most central (**B**) on the unadjusted monovalent vaccine map.

3. Analyses of published data sets

3.1. Antigenic maps of previously published data sets

3.1.1. Previous methods for antigenic characterization

Both monoclonal and polyclonal antibodies have been used for antigenic analyses of DENV. Monoclonal antibodies have been effectively used to identify distinct as well as conserved antigenic structures among DENV types, most often epitopes that are unique to each DENV type, or epitopes conserved across DENV types. However, some anti-DENV monoclonal antibodies recognize epitopes that are neither type-specific nor cross-reactive, exhibiting either differential neutralization of genotypes of the same type or strong neutralization only two or three DENV types (*59–63*). However, the relevance of these antigenic structures as recognized by a polyclonal neutralizing response is not clear.

3.1.2. Literature review to identify data sets for analysis with antigenic cartography

The data sets for which we made antigenic maps, described below, are the best available antigenic analyses using primary infection polyclonal antisera of which we know (*12*, *19*, *22*, *27*, *28*, *63*). Authors of those studies found evidence for antigenic variation among genotypes within the DENV types (genotype nomenclatures are included in table S1). Here, we show how antigenic cartography can reveal additional patterns in neutralization than were not described in the original studies.

We did not expect that these data sets would necessarily form good antigenic maps, as the data sets were not designed to optimize triangulation of viruses by well-spaced antisera. Further, there are some limitations in making an antigenic map of natural infection antisera. First, some were taken at various time-points post-infection, which may affect the neutralizing responses. Second, in some of the studies, antisera were selected based on low neutralization responses to heterologous antisera, potentially introducing a bias. Finally, there is the possibility that some antisera were the result of second infections. Despite these limitations, the resulting antigenic maps for both the natural infection and vaccine antisera provide good fits of the data, as demonstrated by the small error lines.

3.1.3. Monovalent vaccine antisera data sets

We analyzed published data from Vasilakis *et al.* (2008) and Durbin *et al.* (2013), who compared neutralization of sylvatic and endemic DENV isolates using antisera from recipients of the monovalent viral components of the TV003 NIH live-attenuated tetravalent vaccine candidate to assess immunity against possible reintroduction of sylvatic strains into human populations (figs. S23 and S24) (*22*, *27*). In both studies, antisera were drawn 42 days post-inoculation, low-passage isolates were used, and neutralization tests were conducted on Vero cells.

The Durbin *et al.* (2013) data set tested antisera from 22 rDEN4Δ30 recipients against 8 sylvatic and endemic DENV4 isolates, which were passaged in C6/36 cells (*27*). Immunofocus reduction was measured on Vero cells, and a reduction of 60% was reported ($FRNT_{60}$). Titers above the limit of detection were fit as one two-fold higher dilution than the last conducted titration (for example, >1:1,280 would be fit as 1:2,560). Only DENV4 antisera were included for making the antigenic map, because there were not enough numeric titrations to accurately position the DENV1 and DENV2 post-vaccination antisera. Two additional data sets were included in the Durbin *et al.* study, but were not used to make antigenic maps. These included a set of antisera from recipients of a DENV4 vaccine candidate that was not further developed, as well as antisera collected from endemic settings one week to four years post-infection.

Durbin *et al.* identified variation in neutralization among the DENV4 vaccine recipients, as well as a positive correlation between neutralization titer and genetic difference between viruses for the majority of antisera. On the antigenic map of the data, antisera form a diffuse cloud around the infecting isolate, and viruses group into three distinct antigenic clusters (fig. S23). As is clear from the short error lines, the antisera recognize differences among isolates consistently. Further, it was possible to use random 50% subsets of the antisera in this data set to position viruses and observe the same clustering of viruses in 8/10 trials.

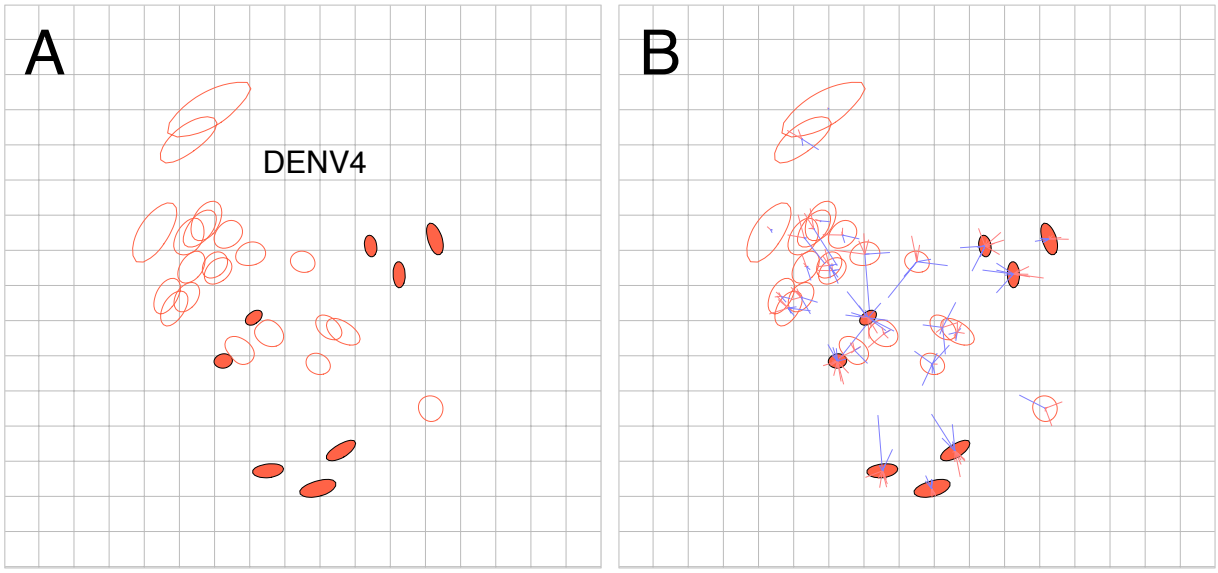

Fig. S23. (**A**) Antigenic map of a data set created by Durbin *et al.* (2013) of 8 genetically diverse DENV4 isolates measured for neutralization with day 42 post-inoculation antisera from rDEN4Δ30 human

vaccine recipients (n=22) (*27*). Viruses were passaged on C6/36 cells, immunofoci were detected on Vero cells, and a reduction of 60% infectivity was reported ($FRNT_{60}$). Grid square sides correspond with a two-fold dilution in the PRNT. (**B**) Error lines are shown.

For the data set from Vasilakis *et al.,* antisera from recipients of rDEN1Δ30 (n=19), rDEN2/4Δ30 (n=18), and rDEN4Δ30 (n=20), were titrated against 12 DENV1, DENV2, and DENV4 isolates of sylvatic and endemic genotypes (*22*). An immunofocus reduction of 80% was reported for the neutralization titer ($FRNT_{80}$). Vasilakis *et al.* identified some variability in the neutralization profiles of vaccine recipients, particularly to the two DENV1 isolates. An antigenic map of this data set demonstrates that antigenic variation within and between types is similar. In particular, the maximum distance among DENV2 isolates is close to the distance to heterologous types, particularly DENV4 (fig. S24 and table S11).

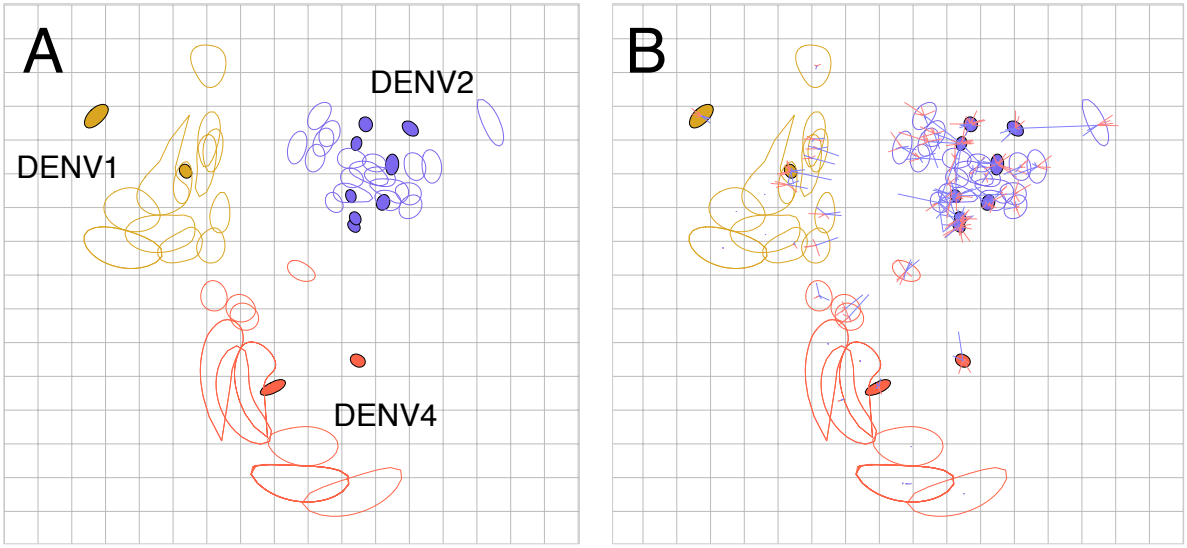

Fig. S24. (**A**) An antigenic map of the data set published by Vasilakis et al. (2008) of sylvatic and endemic DENV1, DENV2, and DENV4 measured with antisera drawn 42 days post-inoculation from human rDEN1Δ30, rDEN2/4Δ30, and rDEN4Δ30 monovalent vaccine recipients (n=57) (*22*). Neutralization tests were conducted on Vero cells and $FRNT_{80}$ titers were reported. Each grid square side is a two-fold dilution in the FRNT. (**B**) Same as A, but including error lines.

3.1.4. Traveler data set

Messer et al. (2012) compared the ability of eleven late-convalescent antisera (2-14 years post-infection) from travelers who had primary DENV1-4 infections in Asia or Latin America to neutralize references viruses for DENV1-4, as well as a panel of molecular clones representing each of the DENV3 genotypes (*28*, *63*). Molecular clones shared genes for the seven non-structural, pre-membrane, and capsid proteins from a DENV3 genotype III parent strain, but had different E genes, representative of the known DENV genotypes. The study is unique in attempting to control for variability among viruses due to differences in in genes other than E. Plasmids were transfected in Vero cells, and resulting viruses were further passaged on Vero cells before the $FRNT_{50}$ (measured as reduction in immunofoci) was conducted on Vero cells. Additional titers published in de Alwis *et al.* (2012) for three of the antisera (DENV1, DENV2, and DENV4) against the reference viruses for DENV1-4 using the same Vero assay were included to make the antigenic map (*63*). All antisera were identified as primary infections responses based on low or undetectable neutralization titers to heterologous DENV types.

The authors found significant differences in the ability of a subset of the traveler antisera to neutralize the different genotypes of DENV3. They observed 19-fold differences across the antisera in ability to neutralize DENV3 isolates by primary DENV3 infection antisera, with one serum only able to neutralize a homologous type isolate at a dilution of 1:15. When we made an antigenic map of this data set, the variation observed within DENV3 is slightly less than the variation observed between types (fig. S25, table S11). There was no effect on the resulting positions when the titrations with the largest error bars from repeat experiments were removed.

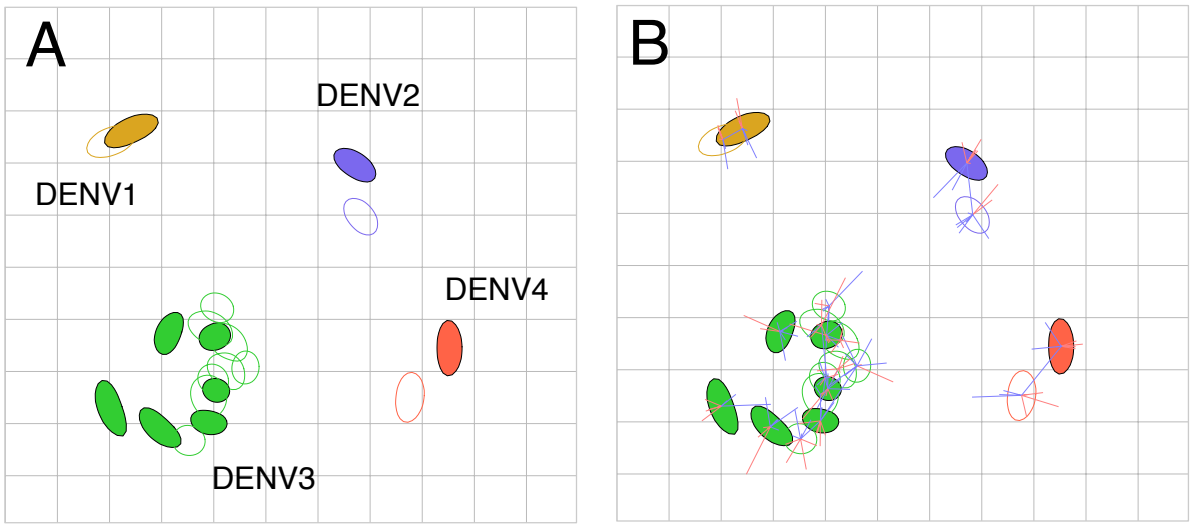

Fig. S25. (**A**) Antigenic map of a data set published by Messer *et al.* (2012) of eleven late-convalescent (2-14 years) primary infection human traveler antisera titrated against representatives of DENV1-4, as well as five molecular clones in which a parent E protein was replaced by E proteins representing each genotype of DENV3 (*28*, *63*). Molecular clones were transfected and passaged on Vero cells, and neutralization tests, with 50% immunofocus reduction tests, were performed on Vero cells ($FRNT_{50}$). The grid denotes a two-fold dilution in the PRNT. (**B**) With error lines.

3.1.5. One year post-inoculation non-human primate data set

Russell and Nisalak (1967) published a seminal paper on the antigenic characterization of DENV using the plaque reduction neutralization test (*12*). They provide a detailed, compelling description of antigenic patterns based on direct interpretation of the neutralization data, and found evidence for antigenic variation within and among DENV types. Their methods are described fully in their publication: briefly, cynomolgus monkeys (*Macaca fascicularis*) were each inoculated with a reference DENV (one for each type) and antisera were drawn one-year post-inoculation. A total of 44 viruses isolated between 1944 and 1967 were titrated against the antisera with a plaque reduction neutralization test on LLC-MK-2 cells (rhesus monkey kidney cells). Fig. S26 is the antigenic map we created of this data set, in which the distance within types is about the same as to a heterologous type for DENV1 and DENV4 isolates.

The optimal orientation of DENV types in this data set differs from that observed in all data sets except the human natural infection map in Fig. 3B, with DENV1 and DENV4 proximal to one another. This may be due to the particular sample of viruses, as well as the availability of only four antisera, which is sufficient, but not optimal, for the coordination of an antigenic map. This limitation is evident in the large confidence areas for some viruses on the map.

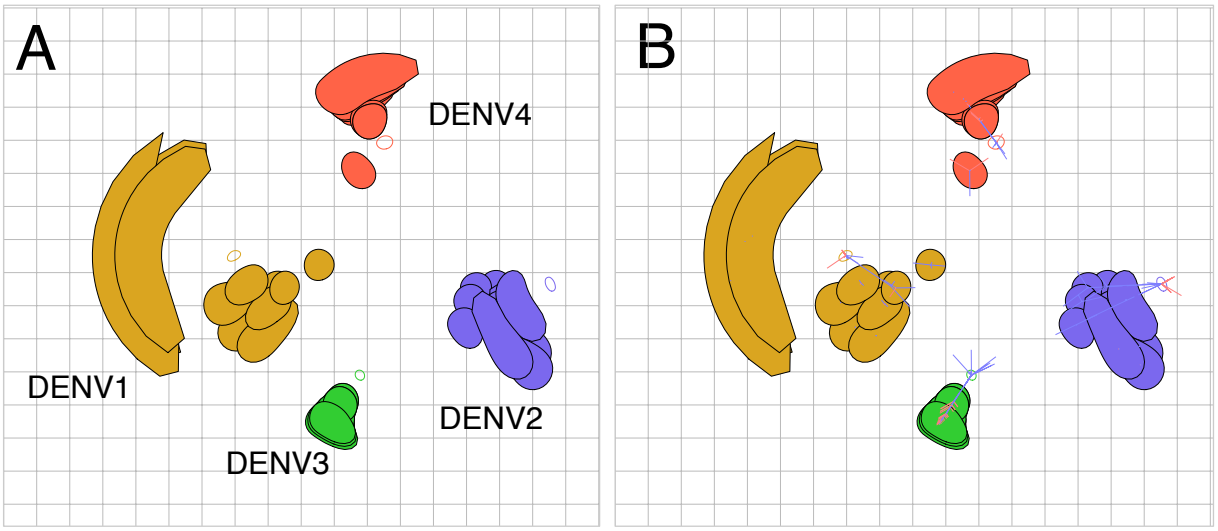

Fig. S26. (**A**) Antigenic map of a data set published by Russell and Nisalak (*12*). DENV isolates from Hawaii, New Guinea, Pakistan, Philippines, Thailand, and Vietnam between 1944-1967 (n=44) were titrated with one-year post-inoculation cynomolgus monkey antisera (n=4), and reported as $PRNT_{50}$ titers. Each grid-square side corresponds to a two-fold dilution in the PRNT. (**B**) Same as A, but with error lines.

3.1.6. Peruvian epidemic antisera data set

A natural occurrence of cross-neutralizing responses was observed in the serological study of an unusually mild DENV2 epidemic that followed a DENV1 epidemic in Iquitos, Peru, as described by Kochel *et al.* 2002 (*19*). The researchers selected a sample of 34 antisera taken during a DENV1 epidemic in 1993-1994 and determined to be monotypic to DENV1, as well as 17 antisera from 1998-1999 during a DENV2 epidemic determined to be monotypic to DENV2. A monotypic response was defined by neutralization titers <1:30 to prototypes of heterologous types, titers >1:60 to the prototype of the homologous type, and absence of detectable IgM antibodies. The viruses they used for screening the sera differed from those used for testing their hypotheses. A plaque assay was conducted on BHK21 cells, and $PRNT_{50}$ titers were reported. They found that DENV1 antisera neutralized DENV1 isolates and American genotype DENV2 isolates better than Asian DENV2 isolates. The DENV2 antisera neutralized both DENV2 genotypes significantly better than DENV1 isolates.

Our antigenic map of the published data shows that the post-infection DENV1 antisera cluster diffusely between the DENV1 isolates and isolates of the American genotype of DENV2 sampled in Peru (fig. S27). Notably, there is antigenic variation between the two American DENV2 genotype viruses (not noted in the original paper), which is comparable to the distance to the Asian genotype DENV2 isolates. The distances between DENV1 and American genotype DENV2 are only slightly greater than the distance between American and Asian DENV2 isolates (table S11).

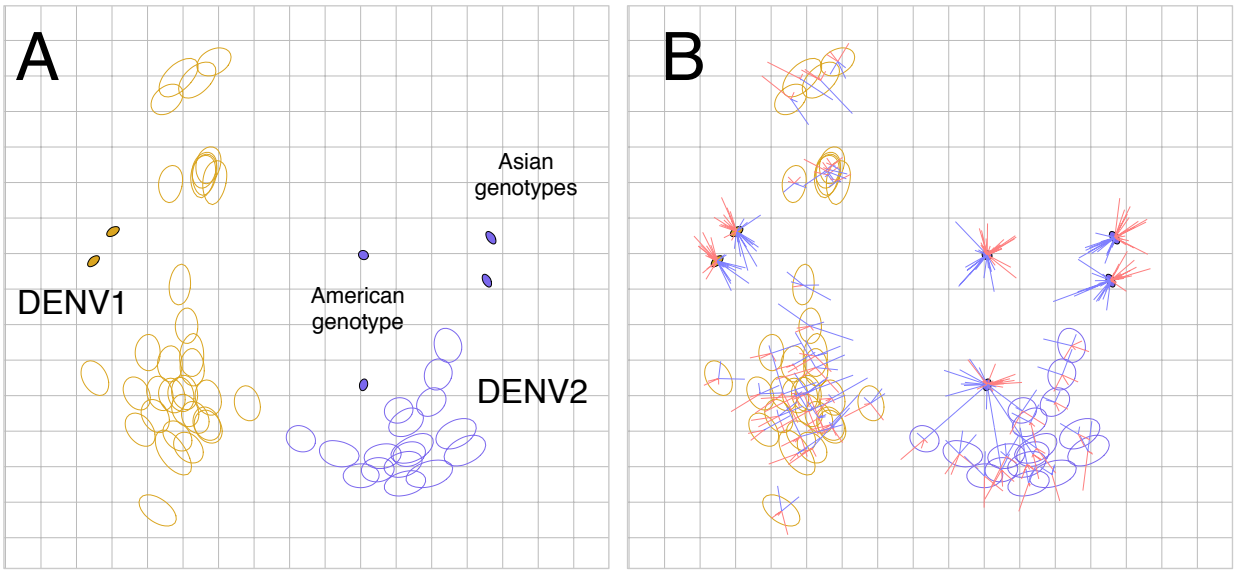

Fig. S27. (**A**) An antigenic map of the neutralization titers from Kochel *et al.* 2002 (*19*). Antisera from 34 individuals identified as DENV1 primary infections and 17 DENV2 primary infections were titrated against two DENV1 isolates, two American genotype DENV2 isolates, and two isolates of Asian genotypes. A lytic immunofocus assay was conducted on BHK21 cells to estimate $PRNT_{50}$ titers. Each grid square side represents a two-fold dilution in the PRNT. (**B**) Same figure as A, but with error lines.

Most of the DENV2 antisera cluster around one of the American DENV2 isolates, and are at similar distances to the all other DENV2 viruses. Overall, the DENV2 antisera are further from DENV1 isolates than most DENV2 isolates, but there is still notable variation in position. Most DENV1 antisera cluster closer to one of the American DENV2 isolates, but a subset is further from that American DENV2, and closer to the other American DENV2 and the Asian DENV2 isolates. Overall, like for individuals inoculated with the same isolate in the vaccine studies, the response of those infected during the Peruvian epidemic vary, but cluster (table S11). The relatively tight clustering observed here on this antigenic map may be the result of a bias in the selection of antisera. DENV1 and DENV2 antisera were selected based on low neutralizing responses to prototypes of the heterologous isolate. This means their responses may be further (depending on the antigenic position of the prototype) from the heterologous type than would be observed if antisera could have been selected based on exposure, not on reactivity.

3.2. Published neutralization titer trajectories

In our literature search, we found that studies documenting the neutralizing responses for up to a year after experimental inoculation and natural infection are consistent with our results; however, this observation was not emphasized in these studies. Heterotypic titers do not wane more than homotypic immunity, even when measured up to a year after infection (*31*, *32*, *64*, *65*).

We analyzed the data for the published studies carefully documenting neutralizing responses for months after experimental inoculation. Hickey *et al.* (2013) experimentally inoculated 16 Rhesus monkeys (four individuals were inoculated with the same virus for each DENV type) and sampled the monkeys every month from 4-13 months after inoculation (*31*). The pattern of neutralizing titers for the NHPs, with accommodation for assay error, is mostly stable over time: the individual monkeys who exhibit early cross-reactive titers to a heterotypic DENV type maintain titers to that type out to the end of the study period (fig. S28).

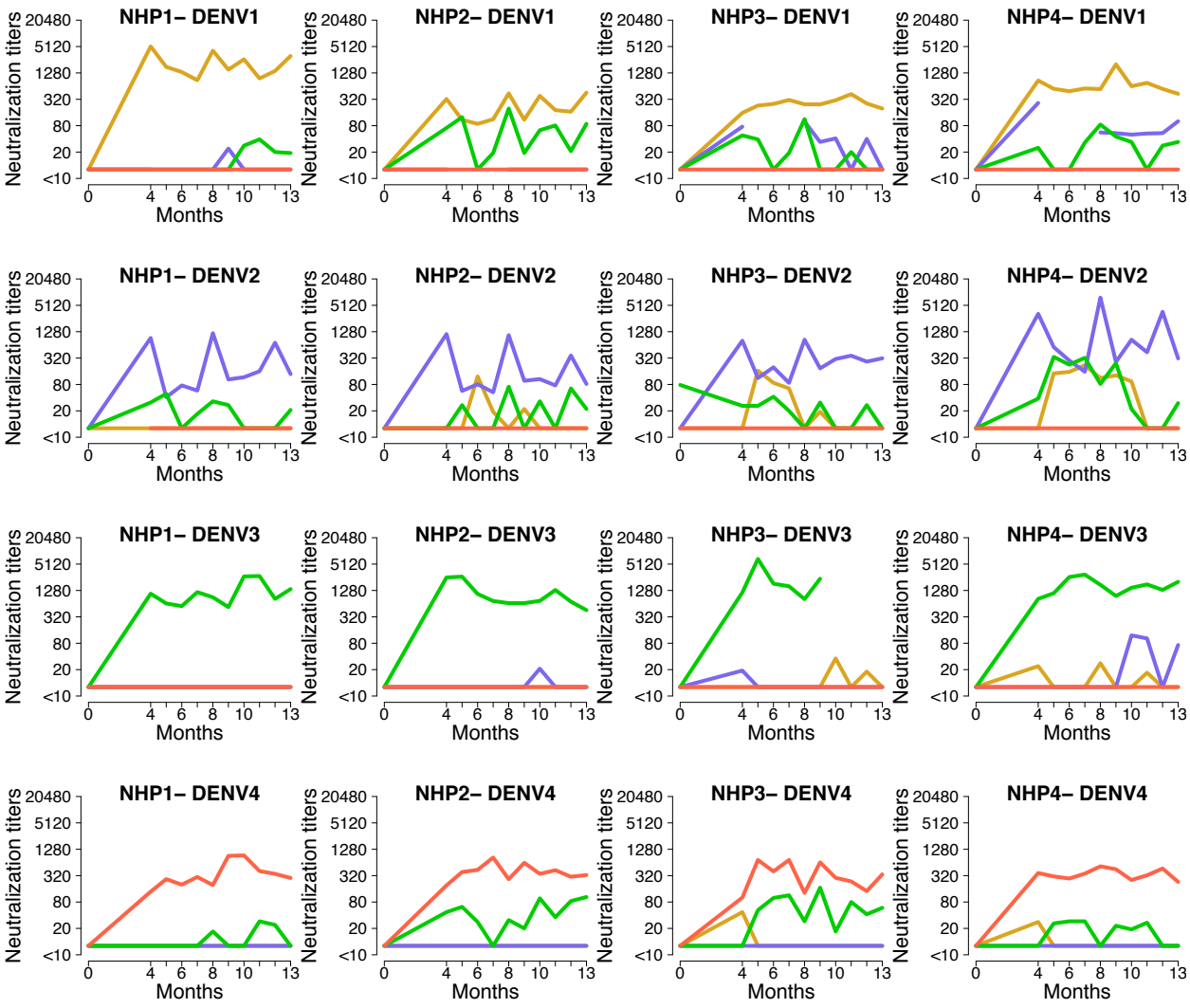

Fig. S28. The trajectories of $FRNT_{50}$ antibody titers of 16 Rhesus monkeys (4 individuals per DENV isolate) from 4-13 months after experimental inoculation against representatives of each DENV type (DENV1=yellow, DENV2=blue, DENV3=green, DENV4=red), published by Hickey *et al.* 2013 (*31*).

In the second study, Kochel *et al.* (2005) measured the neutralizing responses of *Aotus nancymae* monkeys for 1-4 months after experimental inoculation with either DENV1 or one of two genotypes of DENV2 (*32*). The NHPs also shows no evidence of increasing specificity to the infecting type, with titers fluctuating in parallel.

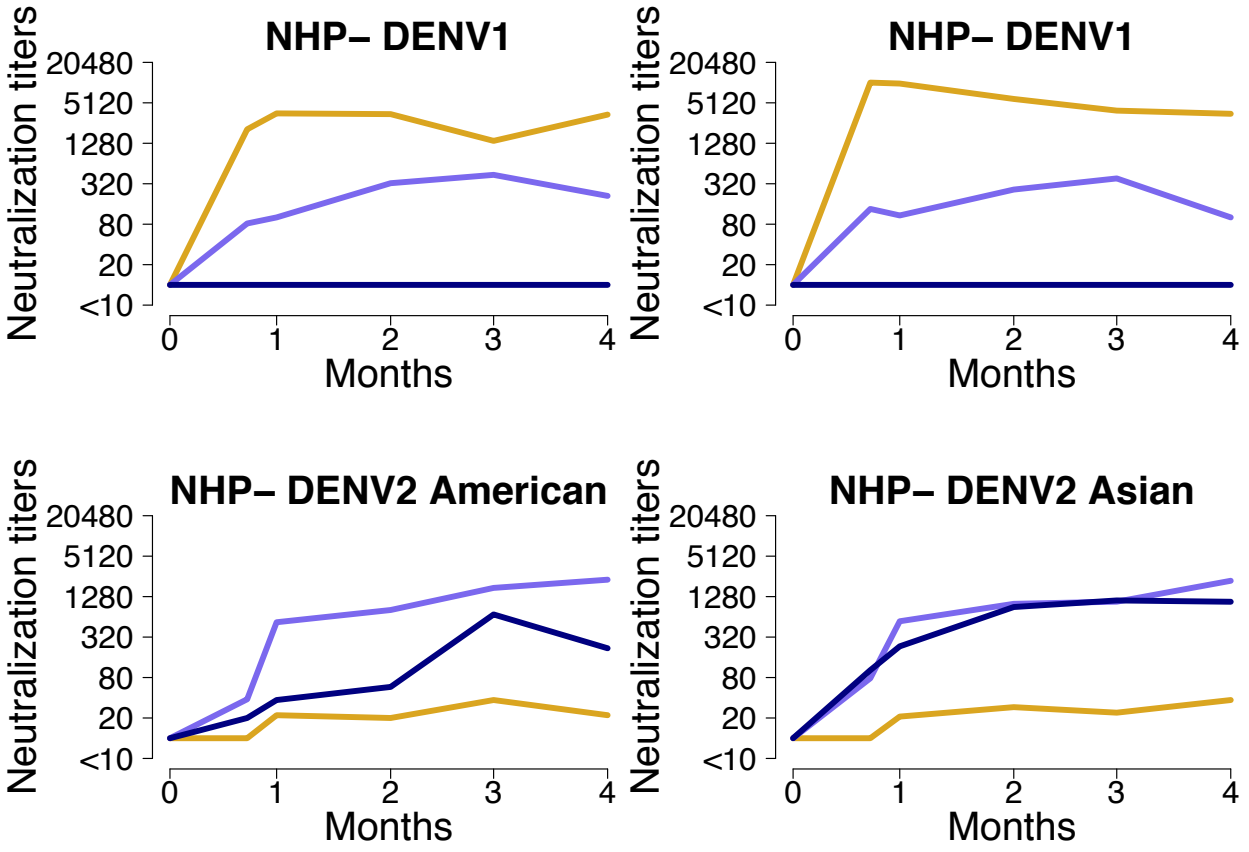

Fig. S29. The trajectories of $PRNT_{50}$ antibody titers of four *Aotus nancymae* monkeys from 0-4 months after experimental inoculation against DENV1 (yellow), American DENV2 (light blue) and Asian DENV2 (dark blue), published by Kochel *et al.* 2005 (*32*).

4. The study of protection and enhancement with antigenic cartography

A major priority of dengue research is to understand the determinants of dengue protection, especially from the severe manifestations of DENV infection, dengue hemorrhagic fever and dengue shock syndrome. Antibody-dependent enhancement (ADE) is central to understanding severe dengue disease and to vaccine development. One property that is hypothesized to relate to ADE is antigenic distance: that within a range of antigenic difference an individual will be protected, but beyond a certain threshold partial antigenic similarity increases the risk of severe disease, whereby antibodies bind but do not protect allowing Fc-receptor mediated infection.

The antigenic maps we present provide a framework for understanding the patterns of neutralization, which up to a certain threshold may correlate with protection. Beyond that point, there may be window of antigenic space where individuals are at highest risk of severe disease. One way to use antigenic cartography and related techniques to study the enhancement threshold is to plot neutralizing and enhancing antibody titers above the maps in a third dimension as an antibody landscape, presented recently by Fonville *et al.* (*66*). The antibody landscape can show the part of antigenic space that poses the greatest risk to an individual.

There are multiple plausible hypotheses about what this enhancement landscape might look like. One is that there is some relationship between the populations of neutralizing and enhancing antibodies, and thus the enhancement landscape would be directly related to the antigenic distances measured on the maps we present here. Alternatively, it is possible that enhancing antibodies constitute a distinct population from the neutralizing antibodies, and the enhancement landscape would have a different shape in relation to the neutralization landscape.

Our work provides a conceptual and quantitative framework to address questions about enhancement and as well as protection, and their relation to viral evolution and dengue epidemiology.

5. The Dengue Antigenic Cartography Consortium

5.1. Description

The Dengue Antigenic Cartography Consortium is an open, global collaboration of dengue researchers who came together to establish how large samples of DENV isolates relate to one another antigenically. The Consortium currently consists of epidemiologists, clinicians, geneticists, cartographers, molecular biologists, government officials, and vaccine developers, based in laboratories in Africa, the Americas, Asia, Europe, and the Pacific. We use antigenic cartography to create antigenic maps, which are high-resolution, quantitative and visual interpretations of neutralization data, providing both accurate measurements of antigenic distances and a visualization that allows for intuitive recognition of antigenic patterns among large samples of viruses. The Consortium is now assembling a panel of diverse DENV isolates and DENV infection antisera to make a globally representative DENV antigenic map. As results from the project become available, they are openly shared with all members of the Consortium.

5.2. Key objectives for Dengue Antigenic Cartography Consortium

1. Continually updated, high-resolution antigenic analyses of DENV should form the basis for an antigenic surveillance system of DENV. A comprehensive antigenic record of DENV will show global antigenic diversity prior to introduction of dengue vaccines, providing a tool for monitoring how antigenically similar vaccine strains are to the viruses that currently circulate endemically, and identifying low-prevalence antigenic outliers that may become endemic.

2. Global antigenic analyses will make it possible to test if antigenic distances among virus populations circulating in specific areas over time are related to local dengue incidence, and if antibody-mediated immunological pressure drives viral evolution. In particular, it will be important to incorporate viruses from regions in which concurrently and consecutively circulating viruses of a homologous type were antigenically distant as well as regions in which viruses of heterologous DENV types were antigenically close, to test if antigenic distances are associated with the magnitude of epidemics.

3. Antigenic cartography will be instrumental for investigating whether antibody neutralization tests that use different methods, cell lines (including those with Fc receptors for measuring antibody-dependent enhancement), and virus preparations, which are known to differ from one another qualitatively, also describe antigenic distances differently among panels of DENV isolates. Experiments in which antisera from individuals with known disease outcome are tested for neutralization of viruses antigenically close and far from the infecting strains may

clarify which techniques measure antigenic differences between viruses that correspond with protection.

4. Antigenic analyses of primary infection non-human primate antisera may help us to parse multi-infection human serological responses. Using antigenic analyses to control for antigenic differences between viruses when analyzing epidemiological and clinical data sets, it may be possible to characterize the breadth of natural infection or vaccine-derived neutralization, as well as test for serological determinants of protection and severe disease that have been difficult to recognize.

5.3. Members of the Dengue Antigenic Cartography Consortium

(Alphabetical by affiliation)

Armed Forces Research Institute of Medical Sciences, Thailand, Stefan Fernandez, Robert Gibbons
Ahmadu Bello University, Nigeria and *University of British Columbia, Canada,* Simon Ayo Yila
University California, Berkeley, USA, Eva Harris, Angela Green, Henry Puerta Guardo, Josefina Coloma, Chunling Wang, Mildred Galvez, Magelda Montoya
University of Buea, Cameroon, Eric Fokam
University of Cambridge, UK, Leah Katzelnick, Judith Fonville, Sarah James, Derek Smith
Erasmus Medical Center, Netherlands, Ron Fouchier, Penelope Koraka, Byron Martina, Albert Osterhaus
University of Ibadan, Nigeria, Adeola Fowotade
Institut Pasteur de Bangui, Central African Republic, Basile Kamgang
Institut Pasteur, Cambodia, Duong Veasna, Ngan Chantha, Huy Rekol, Philippe Buchy
Institut Pasteur, Senegal, Amadou Sall
International University of Africa – Khartoum, Sudan, Mohammed Awadalkareem Ali
Johns Hopkins University, USA, Kaitlin Rainwater-Lovett, Henrik Salje, Isabel Rodríguez, Hannah Clapham, Derek Cummings, Anna Durbin
University of Khartoum, Sudan, Maowia Mukhtar
Kenya Medical Research Institute, Kenya, Rosemary Sang, Yaw Afrane
Kilimanjaro Clinical Research Institute, Tanzania, Reginald Kavishe, Alphaxard Manjurano
University of Lagos, Nigeria, Moses Iorngurum
Mahidol University, Thailand, Sutee Yoksan
University of Maiduguri, Nigeria, David Nadeba Bukbuk
Universiti Malaysia Sarawak, Malaysia, Jane Cardosa
University of Massachusetts Medical School, USA, Irene Bosch
Ministry of Health, Nicaragua, Angel Balmaseda
University of Nairobi, Kenya, Julius Oyugi
National Health Research Institutes, Taiwan, Ih-Jen Su
National Institute of Allergy and Infectious Diseases, USA, Gregory Gromowski, José Bustos Arriaga, Laura VanBlargan, Theodore Pierson, Stephen Whitehead
University of North Carolina, USA, William Messer, Aravinda de Silva
University of Oxford, UK, Jane Messina, Simon Hay
Oxford University Clinical Research Unit, Vietnam, Cameron Simmons

Queensland University of Technology, Australia, John Aaskov
Sudanese Environment Conservation Society, Sudan, Suad Sulaiman
The University of Sydney, Australia, Edward Holmes
University of Texas, USA, Nikos Vasilakis, Robert Tesh
University of Yaounde, Cameroon, Celine Nkenfou
United States Center for Disease Control and Prevention, Puerto Rico, Jorge Muñoz-Jordán
World Health Organization, Switzerland, Joachim Hombach, Raman Velayudhan, Cathy Roth
Walter Reed Army Institute of Research, USA, Melanie Melendrez, Jun Hang, Richard Jarman

6. List of supplementary files

Data file S1. Alignment of E nucleotide sequences for Fig. 1A (Fig1A-aligned-nucleotide-sequences.txt).

Data file S2. PhyML tree for Fig. 1A (Fig1A-phyml-tree.txt).

Data file S3. Bootstrap trees for Fig. 1A (Fig1A-bootrap-trees.txt).

Data file S4. Sequence name key for Fig. 1A (Fig1A-key-for-tree-names-virus-names.txt).

Data file S5. Alignment of E nucleotide sequences for fig. S1 (FigS1-aligned-nucleotide-sequences.txt)

Data file S6. PhyML tree for fig. S1 (FigS1-phyml-tree.txt).

Data file S7. Bootstrap trees for fig. S1 (FigS1-bootrap-trees.txt).

Data file S8. Sequence name key for fig. S1 (FigS1-key-for-tree-names-virus-names.txt).

Data file S9. Excel file including tables S3 – S7 (Tables-S3-S4-S5-S6-S7.xlsx).